Conjugated polymers as promising electrode materials for lithium-ion batteries

Shi, Handa

2024

Shi, H. (2024). Conjugated polymers as promising electrode materials for lithium-ion batteries. Master's thesis, Nanyang Technological University, Singapore. https://hdl.handle.net/10356/182641

https://hdl.handle.net/10356/182641

https://doi.org/10.32657/10356/182641

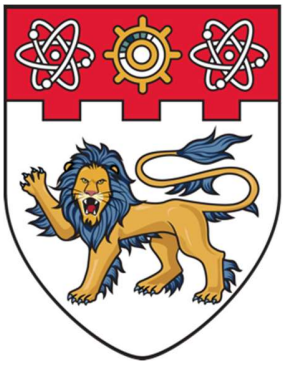

NANYANG TECHNOLOGICAL UNIVERSITY
SINGAPORE

CONJUGATED POLYMERS AS PROMISING ELECTRODE MATERIALS FOR LITHIUM-ION BATTERIES

SHI HANDA

SCHOOL OF MATERIALS SCIENCE AND ENGINEERING

2024

CONJUGATED POLYMERS AS PROMISING ELECTRODE MATERIALS FOR LITHIUM-ION BATTERIES

SHI HANDA

SCHOOL OF MATERIALS SCIENCE AND ENGINEERING

A thesis submitted to the Nanyang Technological University
in partial fulfilment of the requirement for the degree of
Master of Engineering

2024

Statement of Originality

I hereby certify that the work embodied in this thesis is the result of original research, is free of plagiarised materials, and has not been submitted for a higher degree to any other University or Institution.

16/Aug/2024

. . . . . .

Date

. . . . . .

Shi Handa

Supervisor Declaration Statement

I have reviewed the content and presentation style of this thesis and declare it is free of plagiarism and of sufficient grammatical clarity to be examined. To the best of my knowledge, the research and writing are those of the candidate except as acknowledged in the Author Attribution Statement. I confirm that the investigations were conducted in accord with the ethics policies and integrity standards of Nanyang Technological University and that the research data are presented honestly and without prejudice.

16/Aug/2024

. . . . . .
Date

. . . . . .
Prof. Chen Xiaodong

Authorship Attribution Statement

This thesis **does not** contain any materials from papers published in peer-reviewed journals or from papers accepted at conferences in which I am listed as an author.

16/Aug/2024

Shi Handa

. . . . . .
Date

. . . . . .
Shi Handa

Abstract

After the competition of almost half a century, lithium-ion battery (LIB) has become the most important energy storage device in modern society and industry. However, with the still fast-growing demand of batteries with different requirements, such as energy storage device in electric vehicles, traditional inorganic LIBs have exposed their drawbacks, many of the components are toxic and hard to degrade/recycle, lack of the raw resources and high cost in manufacturing process. LIBs with organic materials as electrodes has attracted more interest from researchers under this background. Organic materials as electrode materials have great flexibility in design, because of their rich chemistry in carbon backbones as well as eco-friendly for environmental protection and potentially cost-effective as many organic compounds can be obtained from recycled products and biomass

The main objective of this project is to synthesize novel conjugated polymers as high-performance electrode materials for lithium-ion batteries. All experiments focus on the design, synthesis, characterization, and validation of the electrochemical mechanisms and performance of these materials. Various methods are employed to enhance the battery performance of these materials and to identify the reasons behind their high performance, ultimately leading to new strategies for seeking high-performance electrode materials.

In detail, a brief introduction is provided followed by hypothesis, scope, overview and outcomes of the research. Then, the history of organic materials as electrode materials for rechargeable batteries is reviewed, with a focus on the mechanisms and current research status of conjugated molecules and polymers as electrode materials, highlighting them as the most promising electrodes candidates. Subsequently, various characterization and electrochemical testing methods are introduced in the following chapter to obtain information about the morphology, chemical structure, and electrochemical performance of these polymers as electrode materials, thereby understanding their working principles and enhance performance for further study.

In the first part of the study, two ion-in-conjugation polymers were successfully synthesized, and both demonstrate good performance as cathode materials for LIBs. In the second part of the study, a polymer with a 2D structure was synthesized, and its unique laddered structure greatly enhance the stability as electrode material. Additionally, its distinctive bifunctionality enables it to be applied as both electrodes in LIBs, which exhibits excellent performance in all-plastic battery. Finally, a summary is provided to discuss the results of these polymers and recommendations are proposed for further study and unresolved challenges.

Lay Summary

The aim of this research is to develop novel conjugated polymers for organic batteries and improve their performance to fulfill the requirements for real application. The whole experimental and theoretical work is designed and followed by the synthesis of different conjugated polymers with higher electrochemical performance such as higher conductivity, stability and easier fabrication process. The characterizations are all conducted following the "structure-property strategy" to explain the different properties of the final battery performance on the perspective of the morphology and chemical structures of different polymers. Two major research and findings are well discussed in the following chapters. Then, the outcomes are discussed for the organic battery science community. Future work and outstanding questions are proposed in the last chapter to address the remaining problems for further exploration.

In the first research, two novel ion-in-conjugation polymers are synthesized and applied as cathode materials in lithium-ion batteries. They exhibit superior electrochemical properties and have decent battery performance. This research implicates a new synthesis method of ion-in-conjugation polymers in rechargeable batteries. The research shows that not only the normal six-ring carbon-based materials such as graphite can be electrode materials, but also the ion-in-conjugation materials can have the same capacity, multi-redox center activity and a high conductivity.

Secondly, a ladder-like structure conjugated polymer is synthesized with a 2D structure to strengthen the backbones of this polymer as electrode material to address the soluble problem and low cycle performance. Then the material is applied to fabricate battery cells as electrode materials, both for half-cell (as cathode material) and all plastic cell (as cathode and anode materials) in both electrodes. Results show that the polymer can still exhibit robust stability and performance even in all plastic batteries.

Finally, an overview is discussed the outcomes and impacts of the research. Future work to maximize the potential of conjugated polymers in organic battery is discussed and synthesis strategy is proposed to address the remaining problems for rechargeables batteries.

Acknowledgements

The author appreciates all his previous and current group members and other people who are kind to do a favor during the past two years, without their generous help in academics and life, the author cannot finish the project.

The author first would show great gratitude to his former supervisor associate Prof. Zhang Qichun, who gave the author much freedom to explore science and provided necessary advice as well as the motivation to encourage the author to perform well in this research. His generous help of offering the synthesis of materials and characterization resources inspired the author to think and conclude research scientifically.

The author also received great help and invaluable guidance from current supervisor Prof. Chen Xiaodong. His rigorous and sharp style broaden the mindset of the author to treat science with further mind and always have the will to keep state-of-the-art.

Special thanks are giving to all the staff and colleagues to help the author during the project. Dr. Xie Jian selflessly helped the author to design the whole research process and enhance the performance of the cells, especially during the initial period. Dr. Cao Shengkai provided the author necessary skills in battery fabrication and performance characterization and helps the author in CV test. Dr. He Jinghui assisted the synthesis of the two samples and kindly collected the data of NMR and XRD characterization.

Finally, the author wishes to show his gratitude to his family members. They accompanied the author to overcome a tough period during the past two years. In addition, the guidance and cooperation from the previous group members helped the author a lot to get used to his MEng candidature life.

Table of Contents

Abstract i

Lay Summary iii

Acknowledgements v

Table of Contents vii

Table Captions xi

Figure Captions xiii

Abbreviations xix

Chapter 1 Introduction **1**

1.1 Hypothesis 2

1.2 Objectives and Scope 6

1.3 Dissertation Overview 6

1.4 Findings and Outcomes/Originality 8

References 8

Chapter 2 Literature Review **11**

2.1 Introduction of the Conjugated and Early LIB Electrode Materials 12

2.2 Mechanism of Conjugated Compounds as Electrode Materials 15

2.3 Approaches to Enhance Electrochemical Performance of Conjugated Materials . 18

2.4 Conjugation and Ion-in-conjugation Polymers as Electrode Materials 21

2.5 Summary of literature 27

References 27

Chapter 3 Experimental Methodology 33

3.1 Rationale for selection 34

3.2 Battery Fabrication 34

3.3 Materials Characterization 36

3.3.1 Scanning Electron Microscopy (SEM) 36

3.3.2 Fourier Transform Infrared Spectra (FTIR) 38

3.3.3 Thermogravimetric Analysis (TGA) 40

3.3.4 X-ray Diffraction (XRD) 43

3.3.5 ^{1}H-Nuclear Magnetic Resonance (NMR) and ^{13}C-NMR 44

3.3.6 Elemental Analysis (EA) 45

3.3.7 Energy-Dispersive X-Ray Spectroscopy (EDS) Elemental Mapping 46

3.3.8 Galvanostatic Charge-Discharge 47

3.3.9 Cyclic Voltammetry (CV) 48

3.4 Overview of Methodologies 49

References 50

Chapter 4 Novel Ion-in-conjugation Polymers as Promising Cathode Electrodes for Lithium-ion Organic Batteries 51

4.1 Introduction 52

4.2 Synthesis and Electrochemical Test 52

4.2.1 Synthesis of 1,5-PDAS and 2,6-PDAS 52

4.2.2 Electrochemical Measurements of PDAS 53

4.3 Results and Discussions 53

4.4 Conclusions 62

References 64

Chapter 5 A Laddered Structure Polymer as High-performance Electrodes for Lithium-ion Organic Batteries 65

5.1 Introduction 66

5.2 Synthesis and Electrochemical Test 67

5.2.1 Synthesis of PDB 67

5.2.2 Electrochemical Measurements of PDB 67

5.3 Results and Discussions 68

5.4 Conclusions 78

References 80

Chapter 6 Conclusions and Recommendations 81

6.1 General Discussion 82

6.2 Reconnaissance work not included in main chapters 82

6.2.1 Optimization of PDAS 82

6.2.2 Design of Novel 2D Materials as High Performance Electrode 86

6.3 Outstanding Questions 87

References 89

Table Captions

Table 2.1 Illustration of some typical conjugated molecules and their performance. 14

Table 2.2 Some typical conjugated polymers and polymerized-like COFs as electrode materials 26

Figure Captions

Figure 1.1 A schematic illustration of the recycle and manufacturing process of organic batteries using biomass and resources form the nature. Reproduced with permission from [1]. 2

Figure 1.2 Cell structure and lithium ions, electrons charge transfer in a typical lithium-ion battery. Reproduced with permission from [13]. 4

Figure 2.1 Schematic illustration of benzene molecules with a conjugated carbon ring. 12

Figure 2.2 Schematic illustration of electrochemical redox reaction of PTCDA during lithium intercalation/de-intercalation. 16

Figure 2.3 PTCDA structure and the two step lithiation process 17

Figure 2.4 a) Illustration of synthesis of TPB and its proposed redox reactions. b) Structural formula of NDI and its redox process in LIBs. Reproduced with permission from [31]. 18

Figure 2.5 a) Structure of PDBM and b) PDBS. c) Synthesize route and d) redox reaction mechanism of Li_2PDHBQS. Reproduced with permission from [57]. 24

Figure 2.6 a) Structure of PAQS, PAQxS; b) P14AQ and P15AQ. c) Synthetic route of GPA. Reproduced with permission from [64]. 25

Figure 3.1 Fabrication of the half cells of PDAS-based LIBs and necessary components 35

Figure 3.2 SEM structure illustration. Reproduced with permission from [1]. 37

Figure 3.3 Interaction between specimen and electron beam. Reproduced with permission from [1]. 37

Figure 3.4 Illustration of filament inside the SEM chamber. Reproduced with permission from [1]. 38

Figure 3.5 FTIR instrumental and data analysis. Reproduced with permission from [2]. 39

Figure 3.6 Different molecular vibrations. Reproduced with permission from [2]. 40

Figure 3.7 An example of TGA curves. Reproduced with permission from [4]. 41

Figure 3.8 Schematic illustration of the physical structure of a typical TGA instrument. Reproduced with permission from [5]. 42

Figure 3.9 Diffraction of X-rays through lattices. Reproduced with permission from [7]. 43

Figure 3.10 a) Illustration of the structure of NMR. b) Injection chamber of NMR to insert samples. Reproduced with permission from [8]. 45

Figure 3.11 Illustration of the EA instrument. Reproduced with permission from [9]. .46

Figure 4.1 Synthesis route of 1,5-PDAS and 2,6-PDAS 53

Figure 4.2 SEM image of two polymers. a) 1,5-PDAS; b) 2,6-PDAS 54

Figure 4.3 XRD pattern of 1,5-PDAS (blue line) and 2,6-PDAS (red line) 54

Figure 4.4 FTIR spectra of 1,5-PDAS (a) and 2,6-PDAS (b) 55

Figure 4.5 Weight loss of PDAS during temperature rising in thermogravimetric analysis 56

Figure 4.6 Spectra of 1,5-PDAS and 2,6-PDAS under solid-state ^{13}C-NMR 57

Figure 4.7 Profiles of 1,5-PDAS (left) and 2,6-PDAS (right) during charge and discharge process at the initial cycle 58

Figure 4.8 CV curves of 1,5-PDAS (left) and 2,6-PDAS (right) 59

Figure 4.9 Rate capacity of 1,5-PDAS and 2,6-PDAS under 100 cycles at current density of 20~1500 mA/g 59

Figure 4.10 Cycling performance of 1,5-PDAS and 2.6-PDAS with 100 cycles 60

Figure 4.11 Mechanism of 1,5-PDAS and 2.6-PDAS during discharge and recharge process 63

Figure 5.1 Synthesis route of PDB 67

Figure 5.2 SEM images of pristine PDB and as-prepared PDB 68

Figure 5.3 FTIR profile of PDB 68

Figure 5.4 PDB weight loss under temperature programming 69

Figure 5.5 EDS mapping of PDB from different areas 70

Figure 5.6 Cycle performance of PDB cathodes in $LiPF_6$ in EC/DEC 70

Figure 5.7 Enlarged EIS inset plot of PDB fresh cells with ether-based electrolyte (LiTFSI in DOL/DME) (red) and carbonate-based electrolyte (LiPF6 in EC/DMC) (black) 71

Figure 5.8 a) Mechanism of PDB as cathode b) Charge-discharge profile of PDB c) Cycle performance of PDB in 20 mAh/g d) Rate performance of PDB 72

Figure 5.9 CV profile of PDB 73

Figure 5.10 Ex-situ FTIR analysis of PDB between 3.4-1.5V. a) Galvanostatic charge and discharge profiles at different discharge and recharge status b) FTIR spectra of C=O groups obtained from disassembled cells c) =C-O groups from disassembled cells 74

Figure 5.11 Ultra long cycle performance of PDB 74

Figure 5.12 a) Specific capacity of PDB under different cycles b) Rate performance of PDB c) Cycle performance of PDB 75

Figure 5.13 a) Prelithiation of PDB discharging from 2.8V to 0.005V b) Capacity of CNT additives 75

Figure 5.14 a) Mechanisms of PDB as both electrodes b) Charge-discharge profile of full battery c) Rate performance of the full battery d) Long term cycle performance of full battery 76

Figure 5.15 PDB during redox reaction in charge/discharge process 77

Figure 6.1 The profile diagram of charge and discharge i-V curves of LTO 83

Figure 6.2 The specific capacity of LTO with 1,5-PDAS as binder 84

Figure 6.3 The specific capacity of LTO with 2,6-PDAS as binder 85

Figure 6.4 SEM image of LTO with 1,5-PDAS and the electrode shows excellent flexibility 86

Figure 6.5 Illustration of some porphyrin-like structures and proposed synthesis of 2D frameworks. Reproduced with permission from [2]. 87

Abbreviations

LIB	Lithium-ion Battery
SIB	Sodium-ion Battery
FTIR	Fourier Transform Infrared Spectroscopy
TGA	Thermo Gravimetric Analysis
NMR	Nuclear Magnetic Resonance
XRD	X-Ray Diffraction
SEM	Scanning Electron Microscope
CV	Cyclic Voltammetry
EA	Elemental Analysis
EDS	Energy Dispersive Spectroscopy
MWCNT	Multi-walled Carbon Nanotube
PVDF	Polyvinylidene Fluoride
CNT	Carbon Nanotube
LTO	Lithium Titanate Oxide
DAAQ	Diaminoanthraquinone
SA	Squaric Acid
EC	Ethylene Carbonate
DEC	Diethyl Carbonate
DOL	1,3-Dioxolane
DME	1,2-Dimethoxyethane

Chapter 1

Introduction

This chapter briefly introduces the history of conventional lithium-ion batteries (LIBs) and their substitute organic LIBs. Key parameters with advantages of organic LIBs have been discussed to explain the value and feasibility of this project to investigate novel organic materials for organic LIBs. The hypothesis of chosen materials has been proposed followed by objectives of this project. Finally, overview for the dissertation and the major outcomes are discussed of this research.

1.1 Hypothesis

The invention of high-performance LIBs is one of the most important inventions for modern life. The proliferation of many portable and smart devices such as computers and smartphones would not emerge so fast in the past thirty years without the development of LIBs. As climate change and environmental pollution become important issues spreading on the whole planet, the demand for next-generation LIBs increasingly becomes a promising project at high priority to fulfill the needs of future applications such as electric vehicles generated by electricity and energy storage station applied for green power. With the strong demand in these fields, the next generation of rechargeable batteries should be environmental-friendly and safe with high energy/power density and at the same time have low cost in economics to be applied for sustainable development.[1-2] Researchers have proposed a lot of new rechargeable batteries, such as lithium-sulfur batteries, lithium-air batteries and sodium-ion batteries, or by specifying new electrode materials to further develop the most state-of-the-art LIBs. Various methods are currently being adopted to meet these requirements.[3-12]

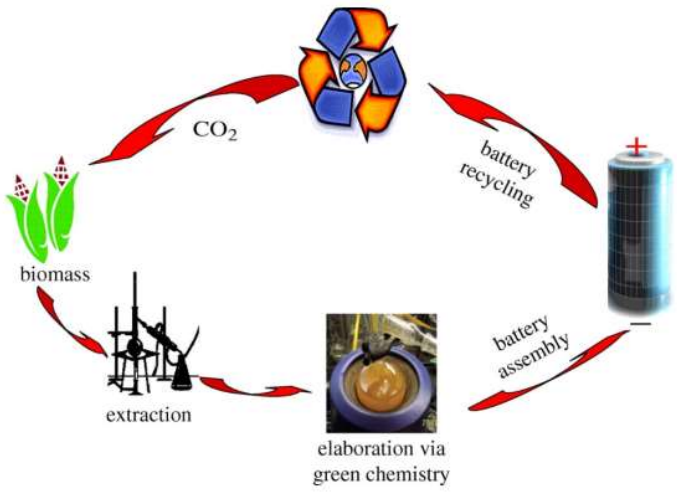

Figure 1.1 A schematic illustration of the recycle and manufacturing process of organic batteries using biomass and resources form nature. Reproduced with permission from [1].

Organic-based materials are one of the potential candidates for electrodes to replace the

current crystalline inorganic LIBs.[13-15] The development of inorganic LIBs has a history of more than one hundred years, and it has gradually matured with the appearance of inorganic compounds capable of lithiation/de-lithiation process with the combination of transitional metal and graphite as cathode and anode materials.[16-17] The first generation of commercial inorganic LIBs use $LiCoO_2$ as cathode materials and over the past decades researchers tried substantial approaches to modify and substitute $LiCoO_2$ with other transition metals compounds or exploring novel structures without Co resources to reduce the cost, next generation lithium ion batteries using $LiFePO_4$ as cathode materials and can approach a capacity of around 170mAh/g while $LiCoO_2$ is only 140mAh/g, lithium titanate $Li_4Ti_5O_{12}$ (LTO) is also proposed to be a good electrode candidate in recent years,[18-20] with the deepening of research, the groundbreaking inventions of these materials to further increase the electrochemical performance is becoming more and more tricky. In addition, high-crystalline structure manufacturing process to achieve decent electrochemical performance and the lack of lithium/nickel resources attribute to high cost of current commercial LIBs, which is one of the biggest hurdles to be applied in emerging different energy storage scenarios. Organic electrode materials are mainly composed of light and cheap elements. This makes it more competitive than transition metal-based inorganic electrode materials, which can be economically friendly and sustainable, while providing high capacity through appropriate material design. Because they are mainly composed of light and cheap elements.[21-22] As shown in Fig 1.1, organic rechargeable batteries can be extracted from natural materials such as biomass, which makes them potentially economic to be used for large scale energy storage systems. The flexibility of the carbon chains of materials inspires infinitive ideas of the molecular design. Moreover, different fabricating routes are expected to find a potentially cost-effective approach for organic materials due to their various properties comparing to conventional inorganic materials, which can be promising as energy device for next generation of flexible electronics. Nevertheless, organic electrode materials still suffer a lot from their poor intrinsic properties in current organic systems of LIBs. Fig 1.2 shows successful organic electrode materials must have redox active sites of charge transfer between cathode and anode.

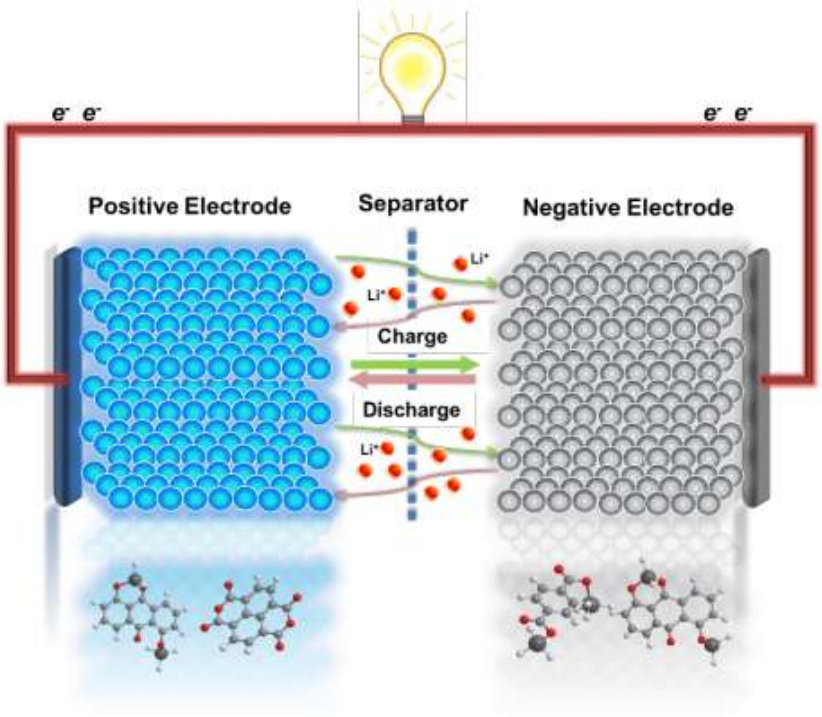

Figure 1.2 Cell structure and lithium ions, electrons charge transfer in a typical lithium-ion battery. Reproduced with permission from [13].

Therefore, different conjugated organic-based materials and various methods to improve their performance are widely studied in this research to make them become better qualified electrode materials. Conjugate polymers are flexible in molecular design and commonly stable in electrochemistry due to their unique ladder chains and π-electrons conjugation. Ion-in-conjugation polymers are investigated with the high interest because some of their novel structures with distinct π-d conjugation while normal conjugated polymers only have π-π conjugation. The ladder-like PDB is also explored in the next research for its 2D structure to avoid the solubility in electrolytes. It is obvious with the continuing effort of the research of novel conjugated organics in rechargeable batteries, people will find these promising organic polymers as high-performance electrode materials for rechargeable batteries.

The research is focused on the designation and development of novel conjugated polymers with decent electrochemical performance, thus, suitable for next generation of organic

rechargeable batteries. The structure of the conjugated polymers is widely investigated during the whole project discussion and characterization conducing, which is the key parameter attributing to excellent electronic conductivity and stability. Research found that ion-in conjugation polymers such as polysquaraines, polysquaramides[23-24] can have highly fragmented fragments with ions and can be used as good electrode materials for rechargeable batteries. The excellent electrochemical performance comes from the small HOMO/LUMO gap, high efficiency in absorbing photon, good crystal properties, and delicate correlation with polar molecules. They can be used as good electrode materials for rechargeable batteries.[25-26]

In addition, the research pays much attention on the optimization of the electrochemical performance of the cells by nanotechnology. Electrode materials with nanostructures are widely used in the project such as MWCNTs to replace traditional carbon black, and nanostructured PDAS and PDB precursors are prepared during the synthesis to enhance their performance. Electrode materials can have many advantages attributing to the nanostructures: (1) they can enlarge the contact areas between the framework of the electrode and electrolyte to reduce polarization loss during battery recharging; (2) diffusion distance is largely decreased during nanotechnology, electrode materials with much heterostructures make electrons and ions travel faster through the electrodes.

Rechargeable batteries with high stability, good conductivity, low weight density and environmentally friendly are intended to achieve with the combination of nanotechnology and insoluble conjugated polymers. Their unique characteristics even makes them possible to be applied as active binder to enhance battery performance in lithium titanate cells. Specially, PDAS has one four-membered ring in each unit, this research will verify the active centers of carbonyl groups in four-membered ring are as the same as six-membered ring, thus, polymer with four-membered ring with active centers (carbonyl group or N atoms, etc.) are potentially with higher energy density due to its simple structure. While on the other hand, laddered structured PDB with -C-S-C- bonds shows excellent stability and performance in LIBs. In general, it is valuable to design and synthesize conjugated polymers as electrode materials for rechargeable batteries, which

can help us better understand π electrons conjugation and mechanism of conjugated polymers in different electrolytes to design more effective multi-active-centered polymers that can store lithium ions more effectively during recycles to develop higher performance rechargeable batteries.

1.2 Objectives and Scope

The research is focused on the synthesis and characterization of novel ion-in-conjugation polymers 1,5-PDAS and 2,6-PDAS. Half cells are fabricated to test their electrochemical performance as cathode materials and further discuss whether they are suitable for LIBs. Then, the laddered structure polymer PDB is synthesized and their application as electrodes in LIBs is explored. Nanostructured ion-in-conjugation PDAS and PDB with bifunction with a 2D ladder structure are prepared to enhance their battery performance and have a better understanding of these polymers. After successful one-step condensation of the polymers, different characterizations are conducted to discuss the morphology of their structures and intrinsic properties. Battery test is conducted for the feasibility of the different polymers as anode or cathode materials in LIBs, respectively. Different salts with electrolyte systems and fine tune of the ratio of different electrode material formulas are well studied to achieve the best battery performance.

1.3 Dissertation Overview

The thesis addresses the strategy and exploration of synthesis of novel conjugated polymers, which provides a broaden research scope of their application in organic rechargeable batteries. The methodology and characterization are conducted to compare the morphology and structure in nanoscale for the understanding of their electrochemical properties, especially in lithium-ion intercalation and de-intercalation. Then, outcomes are well discussed to verify the hypothesis and new synthesis strategies are proposed. Finally, challenges and future work are enumerated for further study.

Chapter 1 provides a brief introduction of the research topic. The objective and meaning

of the exploration are discussed. An overview of the whole research is listed following by the results and unsolved problems in this field for further study.

Chapter 2 reviews the development of organic materials in battery systems. The timeline of organic materials from conducted polymers to conjugated polymers is listed, following by the mechanism and strategies to enhance the performance of these materials. Finally, some novel conjugated materials are discussed in decades.

Chapter 3 discusses the methodology and rationale for every selected characterization for best understanding of the synthesized organic polymers. Several electrochemical approaches are also elaborated for the exploration of cell performance, such as rate capacity, cycle performance and energy efficiency.

Chapter 4 elaborates the synthesis of two novel ion-in-conjugation polymers following by the intact characterization of their properties and morphology. Then, they are applied as cathode materials in LIBs and the performance is tested and results and discussions are discussed in the last part.

Chapter 5 elaborates the successful design and synthesis of a ladder-like structure 2D polymer and the following characterization proves the stability and mechanism of its structure in battery electrodes. Further battery experiments are conducted to test its performance, and the results are discussed later.

Chapter 6 summarizes all the experimental results and literature review, followed by two sections that provide a detailed discussion of their conclusions. Future works are also discussed in the reconnaissance work chapter such as application of the polymers as binder in LIBs. The summarized strategy and potential new synthesis routes are discussed in the last chapter to synthesize polymer networks for organic electrode materials with better performance in the future study.

1.4 Findings and Outcomes/Originality

Conjugated polymers may exhibit decent electrochemical performance to be applied as electrode materials in LIBs, they exhibit high conductivity, decent battery performance considering their theoretical capacity. The differences between 1,5-PDAS and 2,6-PDAS such as crystallinity, and the dithioether interaction of laddered structure -C-S-C bonds to stabilize PDB may also offer perspective to observe the relationship between different performance and different structures in polymers, which broaden the strategy to design better conjugated polymers as electrode materials in the future.

However, conjugated polymers as organic electrode materials still suffer a lot from its low consistency during battery performance test, they may have lower and steep voltage platform (lower energy density) and endurance (poor performance in fast charging) comparing to high-crystalline stable inorganic compounds. In addition, the instability (e.g. four-membered ring in PDAS) chemical structures may deactivate some active functional groups to decrease its electrochemical performance.

References

[1] M. Armand, J.-M. Tarascon. *Nature*. **2008**, 451, 652-657.
[2] N. S. Lewis. *Science*. **2016**, 351.
[3] H. Kim, H. Kim, Z. Ding, M. H. Lee, K. Lim, G. Yoon, and K. Kang. *Advanced Energy Materials*. **2016**, 6, 1600943.
[4] H.-D. Lim, B. Lee, Y. Bae, H. Park, Y. Ko, H. Kim, J. Kim, and K. Kang. *Chemical Society Reviews*. **2017**, 46, 2873-2888.
[5] A. Rosenman, E. Markevich, G. Salitra, D. Aurbach, A. Garsuch, and F. F. Chesneau. *Advanced Energy Materials*. **2015**, 5, 1500212.
[6] T. Ogasawara, A. Débart, M. Holzapfel, P. Novák, and P. G. Bruce. *Journal of the American Chemical Society*. **2006**, 128, 1390-1393.
[7] X. Ji, K. T. Lee, and L. F. Nazar. *Nature Materials*. **2009**, 8, 500-506.
[8] R. Berthelot, D. Carlier, and C. Delmas. *Nature Materials*. **2011**, 10, 74-80.

[9] S. W. Kim, D. H. Seo, X. Ma, G. Ceder, and K. Kang. *Advanced Energy Materials*. **2012**, 2, 710-721.

[10] P. G. Bruce, S. A. Freunberger, L. J. Hardwick, and J.-M. Tarascon. *Nature Materials*. **2012**, 11, 19-29.

[11] B. Dunn, H. Kamath, and J.-M. Tarascon. *Science*. **2011**, 334, 928-935.

[12] S.-K. Jung, H. Kim, M. G. Cho, S.-P. Cho, B. Lee, H. Kim, Y.-U. Park, J. Hong, K.-Y. Park, and G. Yoon. *Nature Energy*. **2017**, 2, 1-9.

[13] T. B. Schon, B. T. McAllister, P.-F. Li, and D. S. Seferos. *Chemical Society Reviews*. **2016**, 45, 6345-6404.

[14] Y. Liang, Z. Tao, and J. Chen. *Advanced Energy Materials*. **2012**, 2, 742-769.

[15] Z. Song, H. Zhou. *Energy & Environmental Science*. **2013**, 6, 2280-2301.

[16] J.-M. Tarascon, M. Armand. *Materials for Sustainable Energy*. **2011**, 171-179.

[17] J. B. Goodenough, Y. Kim. *Chemistry of Materials*. **2010**, 22, 587-603.

[18] H. Li, Z. Wang, L. Chen, and X. Huang. *Advanced Materials*. **2009**, 21, 4593-4607.

[19] C. Li, H. Zhang, L. Fu, H. Liu, Y. Wu, E. Rahm, R. Holze, and H. Wu. *Electrochimica Acta*. **2006**, 51, 3872-3883.

[20] K. Shaju, G. S. Rao, and B. VR, Chowdari. *Electrochem. Acta*. **2002**.

[21] D. Larcher, J.-M. Tarascon. *Nature Chemistry*. **2015**, 7, 19-29.

[22] P. Poizot, F. Dolhem. *Energy & Environmental Science*. **2011**, 4, 2003-2019.

[23] X. F. Cheng, E. B. Shi, X. Hou, J. Shu, J. H. He, H. Li, Q. F. Xu, N. J. Li, D. Y. Chen, and J. M. Lu. *Advanced Electronic Materials*. **2017**, 3, 1700107.

[24] X.-F. Cheng, J. Li, X. Hou, J. Zhou, J.-H. He, H. Li, Q.-F. Xu, N.-J. Li, D.-Y. Chen, and J.-M. Lu. *Science China Chemistry*. **2019**, 62, 753-760.

[25] Y. Chen, M. Tang, Y. Wu, X. Su, X. Li, S. Xu, S. Zhuo, J. Ma, D. Yuan, and C. Wang. *Angewandte Chemie*. **2019**, 131, 14873-14881.

[26] Y. Wu, Y. Chen, M. Tang, S. Zhu, C. Jiang, S. Zhuo, and C. Wang. *Chemical Communications*. **2019**, 55, 10856-10859.

Chapter 2

Literature Review

This chapter retrieves the development of novel organic materials applied as electrode materials in rechargeable batteries. The basic conceptions of conjugated systems have been introduced. Different types of materials and their performance have been discussed chronologically. Mechanisms of different organic materials are demonstrated and followed by the approaches to enhance their electrochemical performance. Conjugated polymers are introduced with highest significance to explain they are the most promising alternatives for organic LIBs in the last section.

2.1 Introduction of the Conjugated and Early LIB Electrode Materials

The conjugated double bond system, that is, the molecular structure of alternating double bonds and single bonds, produces a conjugation effect. The characteristic of the conjugation effect is that the polarization of the chemical bond can be transmitted far along the conjugation system. For example, the result of conjugation is the delocalization of electrons. In the conjugated system, single bonds become shorter and double bonds become longer, and the difference in length between single and double bonds decreases or even disappears. Such a system is relatively stable. For example, the six carbon-carbons in the benzene molecule are all 1.39A, while the bond length of the ordinary carbon-carbon double bond is 1.34A, and the carbon-carbon single bond is 1.48A. So, benzene molecule is more stable than cyclohexene molecule. Benzene molecule has a typical conjugated structure, each carbon center has one electron in the p_z orbital, which is perpendicular to the other three sigma-bonds as shown in Fig 2.1. In addition, the adjacent p_z orbitals overlap each other and a delocalization of π electrons can across the orbitals. In $H_2C=CH_2$, the range of motion of the two π electrons of the π bond is limited between two carbon atoms, which is called localized motion. Conjugation effect reduce internal energy, tending to average bond length, increasing refractive index, and making the entire molecule more stable.

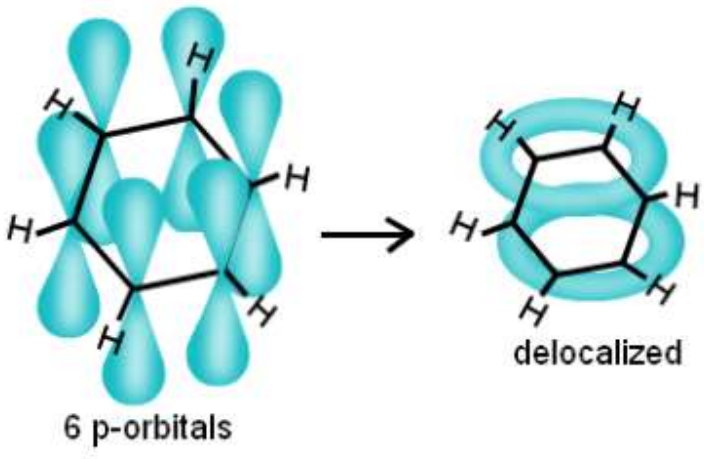

Figure 2.1 Schematic illustration of benzene molecules with a conjugated carbon ring

The first organic electrode materials used for LIBs can be retrieved to 1960s, when researchers found dichloroisocyanuric acid have active electrochemical performance in primary Li battery[1]. Since then, many different types of organic materials have been designed as electrode materials and even in rechargeable lithium batteries. Early research focused on finding electrochemically active molecules and find out their active centers, this is due to majority of the organic materials especially polymers, are nonconductive and have little electrochemical properties. These molecules can be mainly divided into four categories.

The first category is conducting polymers[2], since these polymers have been proved with decent conductivity, their potential to be applied in LIBs are widely investigated. Polymers such as polyacetylene (PAc)[3-5], polythiophene (PTh)[6], and polyaniline (PAn)[7-8] all exhibit reversible electrochemical activity in LIBs. These polymers can be both cathode or anode materials by coating into p-type (generally 3.0V-4.0V vs. Li/Li^+) or corresponding n-type. Coating is essential for conducting polymers to be applied as electrode materials and the self-discharging makes it hard to work in a long term and rechargeable cells. Organosulfur compounds are another important type of organic electrode materials. The most important characteristic of these compounds is their much higher specific capacity (up to 400mAh/g). Tetraethylthiuram disulfide (TETD)[9-10], along with other typical polymers, i.e., poly(2,5-dimercapto-1,3,4-thiadiazole) (PDMcT)[11-12] and poly (5,8-dihydro-1H,4H-2,3,6,7-tetrathia-anthracene) (PDTTA) are chronologically synthesized by researchers, however, those polymers almost none have good cyclability for rechargeable cells[13]. Another category belongs to radical polymers, which have a radical in their neutral state. Radial structure gave the polymers an excellent rate capacity due to their fast charge transfer. Typical polymers such as poly(2,2,6,6-tetramethyl- piperidenyloxyl-4-yl methacrylate) (PTMA)[14-15], poly(2,2,5,5-tetramethyl-3-oxiranyl-3-pyrrolin-1-oxyl ehtylene oxide) (PTEO)[16], and poly(galvinoxylstyrene) (PGVS)[17]. Radial polymers have unsatisfactory specific capacity due to large repeating units that do not have electrochemical activity.

To combine high capacity and without the loss of rate capacity and stability as electrode materials in LIBs, conjugated compounds have been investigated since 1969[1]. These

compounds soon become the most widespread studied organic materials in organic LIBs. The simplest conjugated molecules investigated was benzoquinone (BQ)[18] with the highest theoretical capacity at 496 mAh/g but easiest to dissolve in organic electrolytes. Similarly, anthraquinone (AQ) was investigated as it has more complex structure to avoid dissolution[19-21]. Quinone molecules are suitable to be applied as cathode materials, their voltage platform is larger than 2.0V vs. Li/Li^+. Laddered conjugated molecules with longer chain is studied to overcome dissolution but those molecules are utilized as anode materials due to much lower voltages. Table 2.1 shows some typical conjugated molecules and their performance as electrode materials in LIBs.

Table 2.1 Illustration of some typical conjugated molecules and their performance

Name	**Structure**	**Discharge voltage vs. Li/Li^+**	**Discharge capacity**	**Ref**
Dilithium terephthalate (Li_2TP)	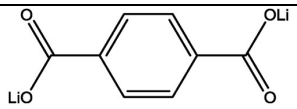	0.8	300	22
Riboflavin (RF)	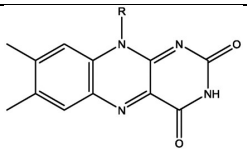	2.65/2.4	105.89	23
N,*N*′-Bis(*n*-propylacetyl)-perylene-3,4,9,10-tetracarboxylic diimide (PDI)	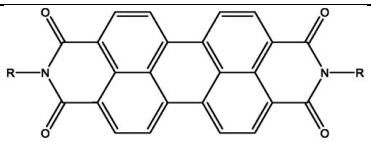	2.16/1.64	77	24
Me_2-BQ	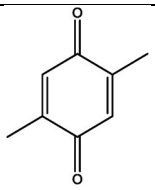	2.5	226	25
1,4,5,8-Naphthalenetetracarboxylic dianhydride (NDA-4N)	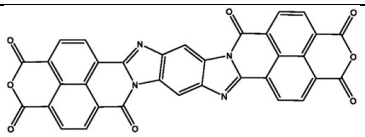	2.9/2.6	141.8	26

2.2 Mechanism of Conjugated Compounds as Electrode Materials

The redox mechanism of conjugated molecules with carbonyl groups as their active centers can simply be described as the enolation reaction of the carbonyl groups. Carbonyl group changes into monoanion during discharge process and returns to neutral state on recharge process. The key parameter for rechargeable LIBs is the reversible lithiation and delithiation of lithium ions at the oxygen atoms on carbonyl groups when they undergo reduction or oxidation process. The earliest conjugated compounds found to be active as cathode materials is Nonylbenzo-hexaquinone (NBHQ)[27]. Lithium ions need to be lithiated or delithiated reversibly through cathode and anode during the electrochemical reaction. Carbonyl groups will undergo oxidation or reduction along with the transfer of the lithium ions, which makes them possible to play the role as electrodes in a rechargeable battery. To explain the mechanism during electrochemical process, molecules with typical multi carbonyl groups such as 3,4,9,10-perylenetetracarboxylic dianhydride (PTCDA)[28] have been investigated. Fig 2.2 shows during the discharge process, each carbonyl group will receive one lithium ion. Carbonyl groups will turn into anion to form lithium enolate and oxidized. Charing reaction has the reversible process, carbonyl groups will receive electrons and lithium ions will delithiated into anode and the cathode PTCDA will recover to initial state. The successful investigation soon encourages researchers to choose small molecules to figure out the specific mechanism of these compounds with multi carbonyl groups such as benzoquinone (BQ) and anthraquinone (AQ). BQ[18] was found to have the highest specific capacity of 496mAh/g while AQ[19] is 257mAh/g. Both the two molecules are applied as cathode materials and both the two carbonyl groups are observed to participate in redox reaction during the lithiation and delithiation process. However, in conventional carbonate electrolyte system, these molecules will experience a rapid degradation. Coulomb efficiencies were also unsatisfactory because of the heavy dissolution of quinone molecules, which even change the color of the electrolyte soon after several recycles.

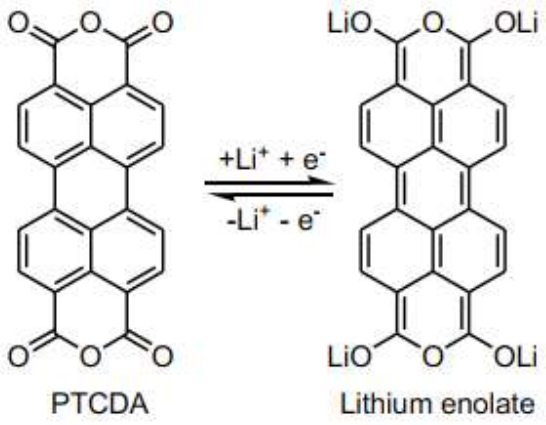

Figure 2.2 Schematic illustration of electrochemical redox reaction of PTCDA during lithium intercalation/de-intercalation.

Carbonyl groups are excellent lithium-ion storage functional groups as active centers during charge/discharge process in rechargeable LIBs, however, as researchers started to design molecules with more carbonyl groups in the backbone of a structure, the performance is not as good as expected, molecules with multi carbonyl groups (typically, more than two carbonyl groups) show less activity comparing to independent ones. This is mainly because of the strong charge impulsion of carbonyl groups after enolation, which makes latter lithium ions harder to intercalate. To utilize the carbonyl groups with high efficiency, many approaches have been studied and result in a novel lithium insertion model, especially in molecules as anode materials[29]. Inspired from the inorganic graphite structure, researchers found out that C6 rings can accept lithium ions reversibly during electrochemical process and form Li6/C6 complex. Molecules with longer carbon chain and more six-membered carbon rings conjugated together has been investigated. 1,4,5,8-naphthalenetetracarboxylic dianhydride (NTCDA)[30] was the first molecule with four carbonyl groups that can absorb more than four lithium ions indicating a new model for lithiation as anode materials. As shown in Fig 2.3, the first step of NTCDA is normal as PTCDA to capture four lithium ions during enolation, however, discharging process with lower voltage researchers found more lithium ions could still intercalated into the material, the unsaturated carbon rings C6 and anhydride ring systems could also be applied for lithiation. The continuous reaction endows PTCDA with super high specific capacity of

1800mAh/g and can fully insert 18 lithium ions during the discharge process Fig 2.3 shows the redox reaction of the PTCDA molecules.

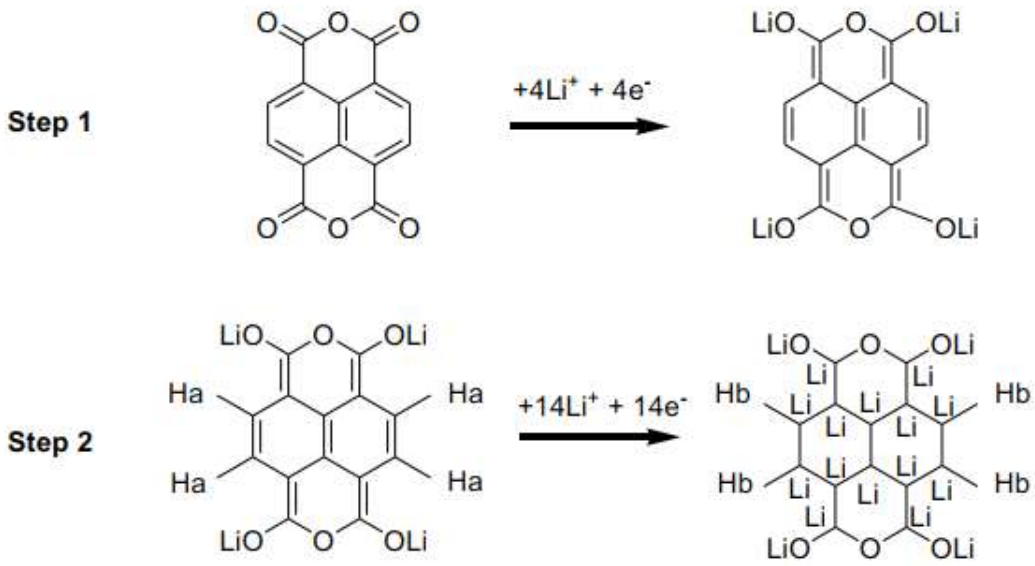

Figure 2.3 PTCDA structure and the two step lithiation process

The new model of C6 rings to absorb lithium ions inspired researchers to design continuing research with longer and bigger chains of conjugated compounds and applied them not only in LIBs but also for sodium-ion batteries, most of these aromatic compounds with C6 rings show amazing performance in electrochemical process. Although these C6-based compounds show excellent performance, their poor cyclability hinders the broader application of commercial usage due to dissolution. Conjugated compounds with insolubility in electrolyte systems is at the highest priority for these conjugated compounds. Some researchers tried to design larger molecules with long chains to avoid the impulsion of carbonyl groups and bond them together to avoid dissolution. One approach is adding big functional group into the backbone of the soluble small molecule, for instance, BQ is easy to dissolve in carbonate electrolyte, but with combining four phthalimide[31] (C8H4NO) groups with benzoquinone to form a compound 2,3,5,6-tetraphthalimido-1,4-benzoquinone (TPB), TPB shows excellent stability and can still reserve 94% of the initial specific capacity of 204mAh/g after 100 cycles at 0.2C. Meanwhile, the carbonyl groups

on the phthalimide groups could also provide extra capacity, but only two carbonyl groups can absorb one lithium ion due to spatial impulsion. Another approach offers an idea to connect small chain molecules one by one and bond them together into a large ring. Many COF (covalent organic framework) molecules are applied as electrode materials using this method and receive excellent cyclability such as NDI (naphthalenediimides). Mono NDI molecule can only reserve 38% of the initial capacity under rate of 1C during discharge process, while triangled NDI molecules can maintain 78% and still exhibit 75% of the theoretical capacity comparing to mono molecules. Fig 2.4 shows the mechanism of the two typical molecules.[31-32]

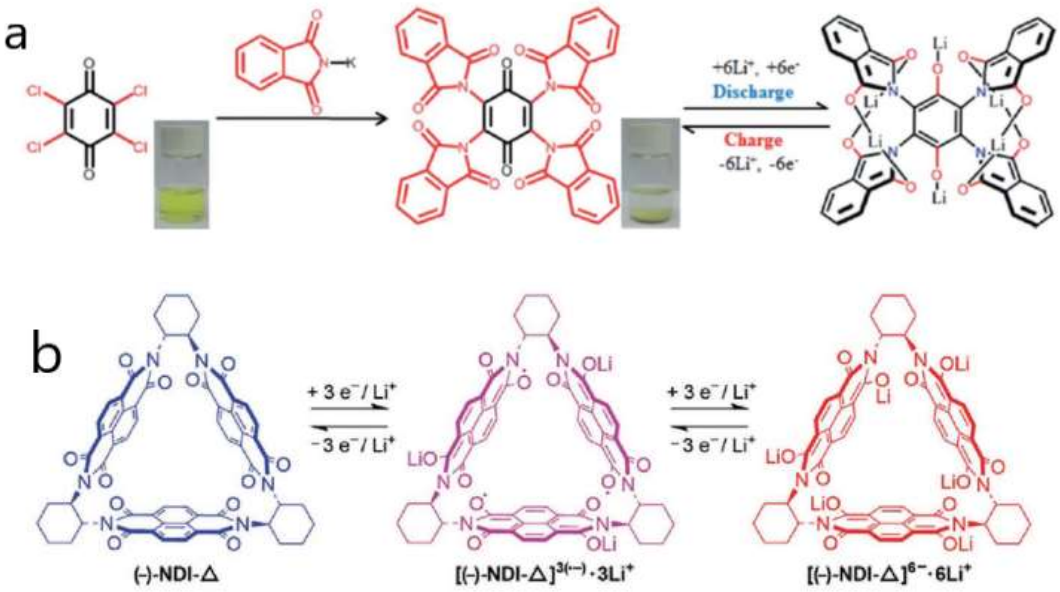

Figure 2.4 a) Illustration of synthesis of TPB and its proposed redox reactions. b) Structural formula of NDI and its redox process in LIBs. Reproduced with permission from [31].

2.3 Approaches to Enhance Electrochemical Performance of Conjugated Materials

Although the excellent electrochemical performance of conjugated polymers gives researchers hope to replace conventional LIB electrode materials. Many problems of organic materials that affect electrochemical performance to be widely studied

in recent years remain unresolved. Many properties such as easy to dissolve in the electrolyte, sluggish kinetics for electrons, and unsatisfactory voltage platforms during discharge/recharge process are still largely hindering their electrochemical performance. The most common and widespread approaches will be discussed in this section to overcome the problems of conjugated compounds.

The most important design starts with the optimization from the molecular level. Due to the flexibility of the organic chemistry, researchers proposed different moderate synthesis routes to adjust the structure and properties of the compounds. The easiest way to change the properties of an organic molecule is to change its functional group. A good way is to change its HOMO/LUMO orbital to adjust its band structure to change the energy level of its band gap.[25, 33]. Researchers got inspiration from biological metabolism and used riboflavin as electrode material[23, 34-35], the molecule have two moderate platforms at 2.65/2.4 V vs. Li/Li^+ during delithiation process. Perylene diimides (PDIs) with strong electronegative groups are also known to have good electrochemical platforms in SIBs[24]. The influence of the functional groups are complicated, the number of substitution[36], position of functional groups[37-38], metal cations[39-40] will all affect the results. Computation also helps to design molecular structure with high performance and choose the optimized functional groups via the calculation of LUMO energies to find compounds with higher energy density[41-45]. Molecular skeleton tuning is another important approach to enhance the electrochemical performance of organic electrode materials. Most active compounds have aromatic rings with conjugated systems, investigation to tune the aromaticity of these compounds are promising to change the electrochemical properties of these molecules. The easiest approach to tune a conjugated material is to extend the conjugation length, which can largely enhance the stability to avoid the dissolution characteristics of organic compounds. The electrical conductivity would also be improved due to the larger conjugated system and the π–π orbital interaction will result in resonance in the conjugated area. Rate capacity will also improve a lot through this elongation[26, 30, 46-47]. For instance, Inatomi *et al*. synthesize two molecules TTP and TTPY, combining double

TTPs and triple TTPYs into new molecules. These so-called 2,5-bis(1,3-dimercapto-2-ylidene)-1,3,4,6-tetrathiopentene and 2,2′ -bis[5-(1,3-Dimercapto-2-ylidene)-1,3,4,6-tetrathiopentene] molecules can still keep conjugated with each other[48-49]. Different approaches have been proposed to tune the skeleton of conjugated compounds such as combine COFs into a ring, NDI triangle molecule is a good example as shown in section 2.3. Other researchers also tried to prepare a porous architecture skeleton to prepare a honeycomb structure polymeric framework to both enhance the stability and rate capacity as porous structure offers larger surface area for lithium ions to transfer during electrochemical process[50]. BPOE is also known as a bipolar porous organic electrode. Its characteristics enable BPOE to be used as both a positive electrode material and a negative electrode material to construct a full-organic cell. In this material, both p-type doping, and n-type doping can be carried out. Inspired by this structure, researchers have developed more bipolar materials, for example, MOP can greatly enhance the rate performance and stability of electrode materials. This type of polymer called microporous organic polymers (MOP) has a large specific surface area because of its porous structure[27]. Recently, COF can be prepared through the characteristics of exfoliation, which greatly shortens its lithium-ion diffusion path. Research has found that the exfoliated COF with a two-dimensional planar structure can reach the nanometer scale and can have good rate performance[51]. Research has found that COF can extremely shorten the migration distance of ions and electrons and promote diffusion, so organic molecules on the surface can be fully utilized, and their exposed active sites can almost achieve 100% participation in redox reactions. Inspired by the exfoliation of COFs, 2,6-diaminoanthraquinone (DAAQ) and 1,3,5-tris(4-formylphenyl)benzene (TFP) are applied as raw materials, these COF nanosheets can be prepared by ball milling and stripping to make 2D ultrathin frameworks. Specific capacity is largely enhanced due to the exfoliation and Li^+ diffusion coefficient also improves to be three times of pristine DAAQ COF molecules.

In this section, different novel approaches have been shown to prove that during

various optimization, conjugated compounds could be as excellent as conventional inorganic materials, thus, promising for the next generation of new LIBs. The rate capacity could be enhanced by the elongation of the skeleton, surface modification of the materials and nanotechnology, robust and functionalized COFs also designed to fabricate organic electrode materials with long cyclability, and high rate capacity than conventional LIBs by exfoliation to get larger surface area.

2.4 Conjugation and Ion-in-conjugation Polymers as Electrode Materials

From the perspective of molecular design, an effective strategy to enhance the insolubility of the small conjugated molecules is by polymerization[52]. Although carbonyl compounds have many advantages, there are still many challenges in the utilization of carbonyl compounds for LIBs. For example, in many energy storage devices, the solubility of conjugated carbonyl compounds in organic electrolytes will cause rapid battery capacity degradation and organic compounds often have lower conductivity and therefore exhibit poor rate performance. Reducing the solubility of conjugated carbonyl compounds and improving the conductivity of conjugated carbonyl compounds are major issues that must be faced in the research design. Polymerization proves its value to solve the solubility of small molecules, so the next section mainly introduces the research progress of conjugated carbonyl polymers.

Polyimide (PI) is an important type of plastic with good high temperature stability and mechanical strength. At present, most of the electroactive monomers of PI are 1,2,4,5-pyromellitic dianhydride (PMDA), 1,4,5,8-naphthalenetetracarboxylic dianhydride (NTCDA) and 3,4,9,10-Perylenetetracarboxylic dianhydride (PTCDA). Based on PI polymer[45], researchers successfully design different polyimides by reacting PMDA and NTCDA with 1,4-phenylenediamine and 1,2-ethylenediamine, respectively. It exhibits high electrochemical activity. Jung *et al*. reported a PI compound with three carbonyl groups synthesized by PTCDA and 2,6-diaminoanthraquinone (DAAQ) and used it as an electrode material for LIBs[53]. This PI compound has a stable charging and discharging platform during the lithiation/delithiation process and can maintain a capacity at 128.43

mAh g^{-1} when it is cycled for 20 cycles and can maintain a Coulomb efficiency of 100% after 280 cycles. In addition, diaminoanthraquinone (DAAQ) as a linker and anhydrides (PTCDA, NTCDA and PMDA) to synthesize a series of PIs compounds through simple chemical reactions is investigated[54]. Among them, when the NTCDA-based PQI-1 compound is used as a positive electrode material for LIBs, it can not only show the electrochemical characteristics of the two monomers at the same time, but also show a higher working voltage. In addition, Sharma *et al*. reported that the imidized PTCDA was prepared with hydrazine hydrate, ethylenediamine, urea, etc., to obtain three different PTCDA derivatives, called hydrazine hydrate-perylene diimide, amine polymer (HP), ethylenediamine-perylene diimide polymer (EDP) and urea-perylene diimide polymer (UP)[55]. By adjusting the composition of the polymer to change the degree of conjugation, the PI compound is inhibited from dissolving in the electrolyte; while extending the degree of conjugation of the organic material, it not only stabilizes the molecular structure, but also improves the conductivity, making electrochemical reaction process exhibits with fast reaction kinetics, and therefore exhibits good electrochemical performance. Hernández *et al*. compared the electrochemical performance of PI polymers synthesized from different acid anhydrides and diamine monomers[56]. By comparison, they found that the redox potential of PI compounds can be adjusted by changing the type of dianhydride precursor. PIs composed of aromatic diamine compounds have better electrochemical performance than PIs composed of aliphatic diamine compounds. At the same time, a polyamide-polyether multi-block copolymer with redox activity was synthesized through the polycondensation reaction between aromatic dianhydride and α-ω-diamino poly(ethylene oxide). This polymer effectively combines ionic conductivity of the polyether block and the redox activity characteristics of the polyamide blocks.

Benzoquinone is currently the most widely studied quinone compound. For example, Gall *et al*. synthesized poly(2,5-dihydroxy-1,4-benzoquinone-3,6-methylene) (PDBM) using 2,5-dihydroxy-1,4-benzoquinone as a monomer. When the polymer is used as a LIBs cathode material, although it exhibits a high theoretical capacity of 705 mAh g^{-1} [57], its rate performance is not satisfactory. This is mainly due to the extremely low electronic conductivity of PDBM, which leads to its slower transfer speed in the lithiation process.

Chloroaniline (CLA) is an organic compound that can be used to react with thioethers to form quinone polymers. Liu *et al*. prepared a poly(2,5-dihydroxy-1,4-benzoquinone sulfide) (PDBS) compound through the reaction between sulfide and CLA. The introduction of ether bonds made the polymer backbone more stable and the carbonyl group exhibits a high degree of reversibility, so PDBS exhibits good cycle stability and rate performance during the electrochemical reaction process[58]. In order to further improve the electrochemical performance of the above-mentioned polymers, Amin *et al*. combined poly(2,5-dihydroxy-1,4-benzoquinone sulfide) (PDHBQS) and carbon nanotubes (SWCNTs) through vacuum filtration. Prepared into a flexible binder-free positive electrode[59]. Its high capacity, good rate performance, excellent cycle stability and good flexibility have laid the foundation for the development of flexible LIBs. Song *et al*. synthesized a new type of quinone-based polymer (poly(2,5-dihydroxy-o-benzoquinone-sulfur)) lithium salt (Li2PDHBQS) through a simple one-step polycondensation reaction[39]. Li_2PDHBQS exhibits good redox reversibility and cycle stability during the electrochemical reaction. When charged to 4.0 V, the lithium ions on Li_2PDHBQS are separated from the carbonyl group, and then undergo a four-electron redox reaction during the subsequent discharge process, thus exhibiting a capacity of higher than 589mAh g^{-1}. Surprisingly, the material exhibited better rate performance and cycle stability after absorbing water than the electrode without water absorption. This may be because the water present in the electrode not only prevents the reaction between the lithium negative electrode and the electrolyte, but also accelerates the transfer rate of lithium ions to the electrode. Fig 2.5 shows some typical derivatives of BQ polymers.

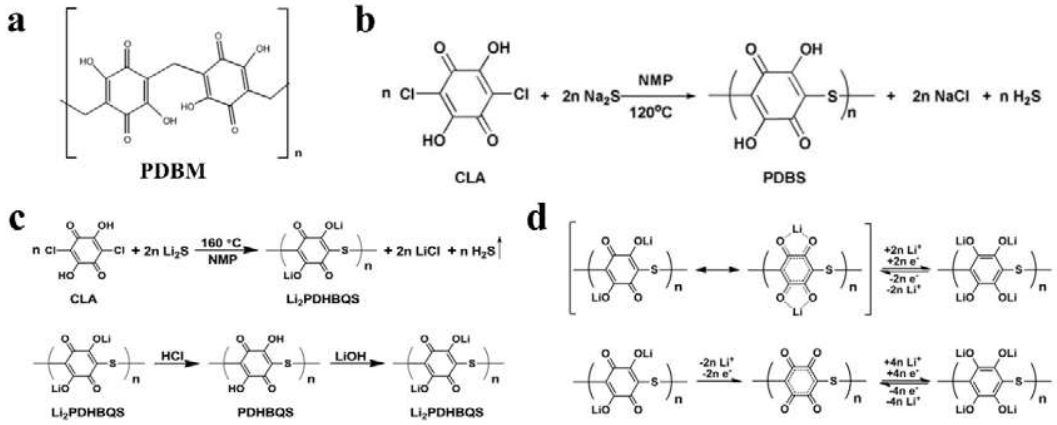

Figure 2.5: a) Structure of PDBM and b) PDBS. c) Synthesize route and d) redox reaction mechanism of Li2PDHBQS. Reproduced with permission from [57].

In addition to benzoquinone, anthraquinone electrode materials have also been extensively studied. Song *et al*. used aromatic halides and sodium sulfide as reactive monomers to synthesize poly(anthraquinone sulfide) (PAQS) and poly(benzoquinone sulfide) electrode materials (PBQS) through a simple polycondensation method[60-61]. This type of polymer has a relatively high molecular weight and degree of conjugation, so as a positive electrode candidate for LIBs, it exhibits excellent cyclability and high reversible capacity. On this basis, Xu's research group and Gomez's research group synthesized PAQS of different molecular weights (PAQ_xS, x=1,2,5,9) (Fig 2.6a)[37, 62] by changing the amount of sodium sulfide in the synthesis process. Interestingly, as the length of the polymer segment changes, the theoretical capacity of PAQ_xS is 2-4 times higher than that of PAQS. However, the linking group used in the polymerization process is not electrochemically active during the electrochemical reaction, so the additional "dead mass" introduced will cause the theoretical capacity to be reduced. Furthermore, Song *et al*.[63] synthesized poly(1,4-anthraquinone) and poly(1,5-anthraquinone) (P14AQ and P15AQ) using the C-C coupling method (as shown in Fig 2.6b) . This method does not introduce inactive linking groups and exhibits a high theoretical capacity. In addition, the polymer P14AQ has a large molecular weight, and the conjugated structure is significantly improved, which helps to improve its cycle stability and rate performance during the electrochemical reaction process. In fact, conjugated carbonyl polymer electrode materials also have the problem of low conductivity, so they often exhibit poor rate performance. To solve this defect, the

introduction of a conductive matrix is also an effective method. Zhang *et al*. synthesized a three-dimensional graphene/PAQS composite gel (GPA) by a dispersion-assembly method, in which PAQS was dispersed on the graphene in a homogeneous way and coated in the graphene sheet (as shown in Fig 2.6c)[64]. The introduction of graphene can effectively enhance the ion affiliation and cyclability of the electrode material. When GPA is used as the LIBs cathode material, it shows a capacity of 156 mAh g^{-1} at a current density of 0.1 C, and the corresponding active material utilization rate has reached 94.9%, and can still maintain 65.4% of the capacity at a current density of 0.1 C at an ultra-high current density of 20 C.

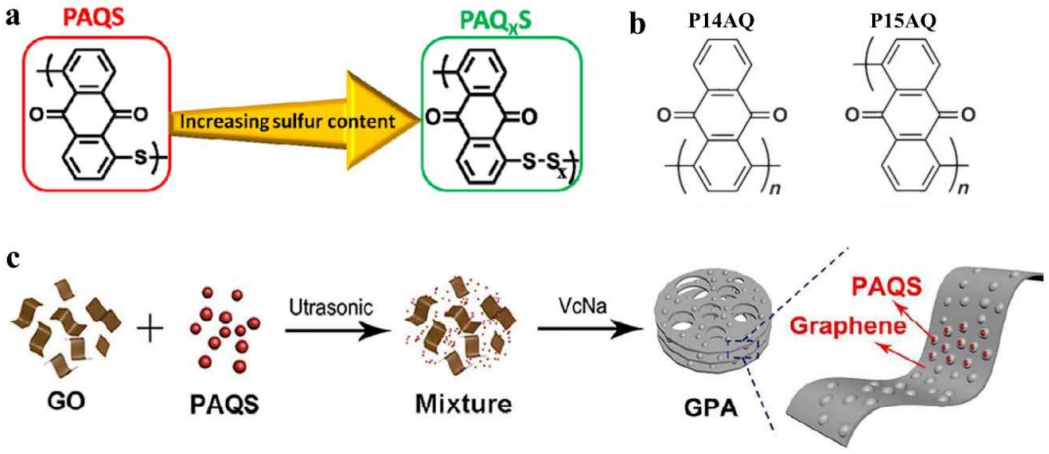

Figure 2.6: a) Structure of PAQS, PAQxS; b) P14AQ and P15AQ. c) Synthetic route of GPA. Reproduced with permission from [64].

In summary, the conjugated carbonyl polymer based on quinone compounds can combine the insolubility of the polymer with electrochemical activity in the quinone structure, so that the electrode material exhibits higher reversible capacity and cycle stability. In addition, the composition and structure of the polymer largely influence the electrochemical performance of organic electrodes. Therefore, in future research of LIBs electrode materials, reasonable molecular design is needed to synthesize more high-performance quinone compounds.

Table 2.2 Some typical conjugated polymers and polymerized-like COFs as electrode materials

Name	Structure	Discharge voltage vs. Li/Li^+ /V	Theoretical/Specific capacity(mAh/g)	Ref
Poly(2,5-dihydroxy-p-benzoquinonyl sulfide) (PDHBQS)	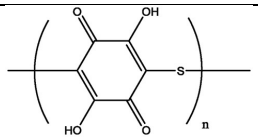	2.7	214	39
Poly(1,5-anthraquinonyl sulfide) (P15AQS)	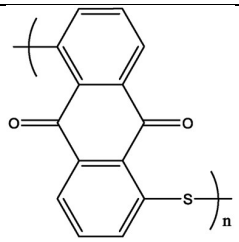	2.19	250	37
Poly(pyromellitic dianhydride) (PMDA)	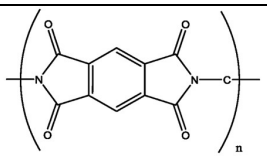	1.73	125	30
1,4,5,8-Naphthalenetetracarboxylic dianhydride (NTCDA)	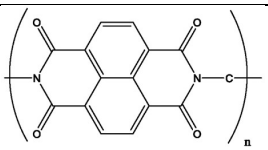	1.89	133	30
Perylene 3,4,9,10-tetracarboxylic dianhydride (PTCDA)	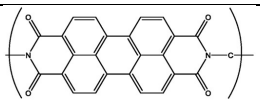	194	112	30
Triformylphloroglucinol (Tp)-diaminobenzo[lmn][3,8] phenanthroline-1,3,6,8(2H,7H)-tetraone (DANT)–COF	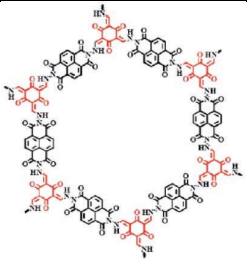	2.3	110	51
PAQI-N14	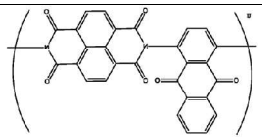	2.15	192	65

2.5 Summary of literature

In this chapter, the history of organic materials, especially the families of conjugated polymers are elaborated from early conducted polymers discovered in 1960s as electrodes in batteries to the state-of-the-art large aromatic molecules in different battery systems. The mechanism, synthesis strategy and approaches to enhance the performance of the batteries are further discussed in the following part. Then, ion-in-conjugation polymers and polymers with more complicated structure are discussed and explain their functionalities to solve the problems of organic batteries.

From the overview of recent study of conjugated polymers, two different kinds of conjugated polymers are synthesized and applied as active electrode materials in LIBs, respectively. Their novelty and mechanisms are well discussed with different characterization methods. Then, an overall discussion is organized to summarize the discovery of these polymers and unsolved challenges are proposed for further study.

References

[1] D. Williams, J. Byrne, and J. Driscoll. *Journal of the Electrochemical Society*. **1969**, 116, 2.

[2] H. Shirakawa, E. J. Louis, A. G. MacDiarmid, C. K. Chiang, and A. J. Heeger. *Journal of the Chemical Society, Chemical Communications*. **1977**, 578-580.

[3] P. J. Nigrey, D. MacInnes Jr, D. P. Nairns, A. G. MacDiarmid, and A. J. Heeger. *Journal of the Electrochemical Society*. **1981**, 128, 1651.

[4] K. Shinozaki, Y. Tomizuka, and A. Nojiri. *Japanese Journal of Applied Physics*. **1984**, 23, L892.

[5] L. Shacklette, J. Toth, N. Murthy, and R. Baughman. *Journal of the Electrochemical Society*. **1985**, 132, 1529.

[6] K. Kaneto, K. Yoshino, and Y. Inuishi. *Japanese Journal of Applied Physics*. **1983**, 22, L567.

[7] A. G. MacDiarmid, L. Yang, W. Huang, and B. Humphrey. *Synthetic Metals*. **1987**, 18, 393-398.

[8] J. Desilvestro, W. Scheifele, and O. Haas. *Journal of the Electrochemical Society*. **1992**, 139, 2727.

[9] S. J. Visco, L. C. DeJonghe. *Journal of the Electrochemical Society*. **1988**, 135, 2905.

[10] M. Liu, S. J. Visco, and L. C. De Jonghe. *Journal of the Electrochemical Society*. **1989**, 136, 2570.

[11] S. Visco, M. Liu, M. Armand, and L. De Jonghe. *Molecular Crystals and Liquid Crystals*. **1990**, 190, 185-195.

[12] M. Liu, S. J. Visco, and L. C. De Jonghe. *Journal of the Electrochemical Society*. **1991**, 138, 1891.

[13] S.-R. Deng, L.-B. Kong, G.-Q. Hu, T. Wu, D. Li, Y.-H. Zhou, and Z.-Y. Li. *Electrochimica Acta*. **2006**, 51, 2589-2593.

[14] S. Barriga. *Synlett*. **2001**, 2001, 0563.

[15] K. Nakahara, S. Iwasa, M. Satoh, Y. Morioka, and J. Iriyama. *Chemical Physics Letters*. **2002**, 359, 351.

[16] K. Oyaizu, T. Kawamoto, T. Suga, and H. Nishide. *Macromolecules*. **2010**, 43, 10382-10389.

[17] T. Suga, H. Ohshiro, S. Sugita, K. Oyaizu, and H. Nishide. *Advanced Materials*. **2009**, 21, 1627-1630.

[18] H. Alt, H. Binder, A. Köhling, and G. Sandstede. *Electrochimica Acta*. **1972**, 17, 873-887.

[19] M. Pasquali, G. Pistoia, T. Boschi, and P. Tagliatesta. *Solid State Ionics*. **1987**, 23, 261-266.

[20] A. J. Wain, G. G. Wildgoose, C. G. Heald, L. Jiang, T. G. Jones, and R. G. Compton. *The Journal of Physical Chemistry B*. **2005**, 109, 3971-3978.

[21] Z. Lei, W. Wei-kun, W. An-bang, Y. Zhong-bao, C. Shi, and Y. Yu-sheng. *Journal of the Electrochemical Society*. **2011**, 158, A991.

[22] M. Armand, S. Grugeon, H. Vezin, and S. Laruelle. *Nature Materials*. **2009**, 8, 120-125.

[23] M. Lee, J. Hong, D. H. Seo, D. H. Nam, K. T. Nam, K. Kang, and C. B. Park. *Angewandte Chemie International Edition*. **2013**, 52, 8171-8171.

[24] H. Banda, D. Damien, K. Nagarajan, A. Raj, M. Hariharan, and M. M. Shaijumon. *Advanced Energy Materials*. **2017**, 7, 1701316.

[25] T. Yokoji, Y. Kameyama, S. Sakaida, N. Maruyama, M. Satoh, and H. Matsubara. *Chemistry Letters*. **2015**, 44, 1726-1728.

[26] J. Xie, W. Chen, Z. Wang, K. C. W. Jie, M. Liu, and Q. Zhang. *Chemistry–An Asian Journal*. **2017**, 12, 868-876.

[27] C. Zhang, X. Yang, W. Ren, Y. Wang, F. Su, and J.-X. Jiang. *Journal of Power Sources*. **2016**, 317, 49-56.

[28] X. Han, C. Chang, L. Yuan, T. Sun, and J. Sun. *Advanced Materials*. **2007**, 19, 1616-1621.

[29] X. Han, G. Qing, J. Sun, and T. Sun. *Angewandte Chemie International Edition*. **2012**, 124, 5237-5241.

[30] H.-G. Wang, S. Yuan, D.-L. Ma, X.-B. Zhang, and J.-M. Yan. *Energy & Environmental Science*. **2015**, 8, 1660-1681.

[31] Z. Luo, L. Liu, Q. Zhao, F. Li, and J. Chen. *Angewandte Chemie International Edition*. **2017**, 129, 12735-12739.

[32] D. Chen, A. J. Avestro, Z. Chen, J. Sun, S. Wang, M. Xiao, Z. Erno, M. M. Algaradah, M. S. Nassar, and K. Amine. *Advanced Materials*. **2015**, 27, 2907-2912.

[33] S. Nishida, Y. Yamamoto, T. Takui, and Y. Morita. *ChemSusChem*. **2013**, 6, 794-797.

[34] J. Hong, M. Lee, B. Lee, D.-H. Seo, C. B. Park, and K. Kang. *Nature Communications*. **2014**, 5, 1-9.

[35] M. Lee, J. Hong, H. Kim, H. D. Lim, S. B. Cho, K. Kang, and C. B. Park. *Advanced Materials*. **2014**, 26, 2558-2565.

[36] S. Gottis, A.-L. Barrès, F. Dolhem, and P. Poizot. *ACS Applied Materials & Interfaces*. **2014**, 6, 10870-10876.

[37] W. Xu, A. Read, P. K. Koech, D. Hu, C. Wang, J. Xiao, A. B. Padmaperuma, G. L. Graff, J. Liu, and J.-G. Zhang. *Journal of Materials Chemistry*. **2012**, 22, 4032-4039.

[38] R. Zeng, L. Xing, Y. Qiu, Y. Wang, W. Huang, W. Li, and S. Yang. *Electrochimica Acta*. **2014**, 146, 447-454.

[39] Z. Song, Y. Qian, X. Liu, T. Zhang, Y. Zhu, H. Yu, M. Otani, and H. Zhou. *Energy & Environmental Science*. **2014**, 7, 4077-4086.

[40] S. Renault, J. Geng, F. Dolhem, and P. Poizot. *Chemical Communications*. **2011**, 47, 2414-2416.

[41] K. Hernandez-Burgos, S. E. Burkhardt, G. G. Rodríguez-Calero, R. G. Hennig, and H. D. Abruna. *The Journal of Physical Chemistry C*. **2014**, 118, 6046-6051.

[42] J. E. Bachman, L. A. Curtiss, and R. S. Assary. *The Journal of Physical Chemistry A*. **2014**, 118, 8852-8860.

[43] C. Karlsson, E. Jämstorp, M. Strømme, and M. Sjödin. *The Journal of Physical Chemistry C*. **2012**, 116, 3793-3801.

[44] S. E. Burkhardt, M. A. Lowe, S. Conte, W. Zhou, H. Qian, G. G. Rodríguez-Calero, J. Gao, R. G. Hennig, and H. D. Abruña. *Energy & Environmental Science*. **2012**, 5, 7176-7187.

[45] X.-Q. Zhu, C.-H. Wang. *The Journal of Organic Chemistry*. **2010**, 75, 5037-5047.

[46] L. Fédele, F. Sauvage, J. Bois, J.-M. Tarascon, and M. Becuwe. *Journal of the Electrochemical Society*. **2013**, 161, A46.

[47] L. Fédèle, F. Sauvage, S. Gottis, C. Davoisne, E. Salager, J.-N. Chotard, and M. Becuwe. *Chemistry of Materials*. **2017**, 29, 546-554.

[48] Y. Inatomi, N. Hojo, T. Yamamoto, S.-i. Watanabe, and Y. Misaki. *ChemPlusChem*. **2012**, 77, 973.

[49] M. Kato, K.-i. Senoo, M. Yao, and Y. Misaki. *Journal of Materials Chemistry A*. **2014**, 2, 6747-6754.

[50] K. Sakaushi, E. Hosono, G. Nickerl, T. Gemming, H. Zhou, S. Kaskel, and J. Eckert. *Nature Communications*. **2013**, 4, 1-7.

[51] S. Wang, Q. Wang, P. Shao, Y. Han, X. Gao, L. Ma, S. Yuan, X. Ma, J. Zhou, and X. Feng. *Journal of the American Chemical Society*. **2017**, 139, 4258-4261.

[52] Y. Liang, Z. Tao, and J. Chen. *Advanced Energy Materials*. **2012**, 2, 742-769.

[53] W. Zhang, P. Sun, and S. Sun. *Journal of Materiomics*. **2017**, 3, 184-190.

[54] B. Tian, G.-H. Ning, W. Tang, C. Peng, D. Yu, Z. Chen, Y. Xiao, C. Su, and K. P. Loh. *Materials Horizons*. **2016**, 3, 429-433.

[55] P. Sharma, D. Damien, K. Nagarajan, M. M. Shaijumon, and M. Hariharan. *The Journal of Physical Chemistry Letters*. **2013**, 4, 3192-3197.

[56] G. Hernández, M. Salsamendi, S. M. Morozova, E. I. Lozinskaya, S. Devaraj, Y. S. Vygodskii, A. S. Shaplov, and D. Mecerreyes. *Journal of Polymer Science Part A: Polymer Chemistry*. **2018**, 56, 714-723.

[57] T. Le Gall, K. H. Reiman, M. C. Grossel, and J. R. Owen. *Journal of Power Sources*. **2003**, 119, 316-320.

[58] K. Liu, J. Zheng, G. Zhong, and Y. Yang. *Journal of Materials Chemistry*. **2011**, 21, 4125-4131.

[59] K. Amin, Q. Meng, A. Ahmad, M. Cheng, M. Zhang, L. Mao, K. Lu, and Z. Wei. *Advanced Materials*. **2018**, 30, 1703868.

[60] Z. Song, H. Zhan, and Y. Zhou. *Chemical Communications*. **2009**, 448-450.

[61] Z. Song, Y. Qian, T. Zhang, M. Otani, and H. Zhou. *Advanced Science*. **2015**, 2, 1500124.

[62] I. Gomez, O. Leonet, J. Alberto Blazquez, H.-J. r. Grande, and D. Mecerreyes. *ACS Macro Letters*. **2018**, 7, 419-424.

[63] Z. Song, Y. Qian, M. L. Gordin, D. Tang, T. Xu, M. Otani, H. Zhan, H. Zhou, and D. Wang. *Angewandte Chemie International Edition*. **2015**, 127, 14153-14157.

[64] Y. Zhang, Y. Huang, G. Yang, F. Bu, K. Li, I. Shakir, and Y. Xu. *ACS Applied Materials & Interfaces*. **2017**, 9, 15549-15556.

[65] F. Xu, H. Wang, J. Lin, X. Luo, S.-a. Cao, and H. Yang. *Journal of Materials Chemistry A*. **2016**, 4, 11491-11497.

Chapter 3

Experimental Methodology

This chapter demonstrates the rationale of several different characterization approaches for conjugated polymers and measurements for battery performance. Battery fabrication process is exhibited to assemble the LIB cells. Specific parameters are illustrated on battery test. SEM, FTIR, TGA, XRD, NMR and EDS characterizations are introduced respectively to determine the structure information of conjugated polymers and some other key parameters that will influence the electrochemical performance are discussed using the methods such as Galvanostatic Charge-Discharge and Cyclic Voltammetry.

3.1 Rationale for selection

Various characterization methods are widely used in this project to ensure the correct synthesis of conjugated samples and characterize the electrochemical properties of the fabricated batteries. FTIR is used to ensure the functional groups of the polymers to ensure the connection site of the raw materials. TGA is used for the thermal stability of the sample to determine whether they are suitable for LIB electrodes. SEM illustrates the topological characteristics of the surface of the polymers and observe how nanotechnology preparation tunes the morphology of the polymers. ^{13}C-NMR demonstrates the carbon backbone structure of the polymer unit to ensure the correct synthesis of the 1,5-PDAS, 2,6-PDAS and PDB with the result of FTIR. XRD illustrates the crystallinity of the two samples to explain the difference to their corresponding electrochemical properties and provides information about π-π staking of the conjugated systems. EA and EDS mapping are used to explore the elemental composition and further indicate the degree of polymerization and information of functional groups in polymers. Neware battery testing system is used for obtaining electrochemical performance of batteries. Specific capacity, rate capacity and Coulomb efficiency and other parameters are tested to obtain the power density, stability, and fast-charging behavior of the materials to determine whether they are suitable for LIBs. CV curve demonstrates the redox information of the polymers. Specific principles of each instrument and their analysis will be elaborated in corresponding section, respectively.

3.2 Battery Fabrication

Fig 3.1 shows the half-cell fabrication process with PDAS samples[1]. Necessary components needed to assemble CR2032 coin cells are listed below. All the parts of a complete CR2032 coin cell including a positive case, a negative case, a separator (Celgard 2400), a stainless steel spacer, a stainless steel spring, a lithium sheet and a copper foil current collector. All the components outside the glovebox of the coin-type cells were cleaned with ethanol and dried in vacuum oven for 24h. The whole assembling process is conducted in a glovebox. Argon gas circulation is needed during the whole process to protect the active components. The moisture and oxygen levels in the glovebox were below

10^{-6}. The anodes were prepared by combination of 30 ωt% with 50 ωt% of multi-walled carbon nanotubes (MWCNTs) and 20 ωt% of polyvinylidene fluoride (PVDF). Put these powder into a mortar and wet the powders with n-methyl-2- pyrrolidone (NMP) solvent. Then mix all the materials in a clean agate mortar washed by ethanol for half an hour until homogeneous slurry is obtained. Then the slurry is homogeneously pasted on aluminum foil (used as current collector). Finally, the wet electrode is placed in vacuum oven for 24h to dry the organic solvent. Counter electrode is Li slice for the half cell. 1 mol/L (M) lithium bis(trifluoromethanesulfonyl)imide (LiTFSI) in 1,3-dioxolane (DOL) and dimethyl ether (DME) (1/1, v/v) were used as electrolyte systems for the half cell.

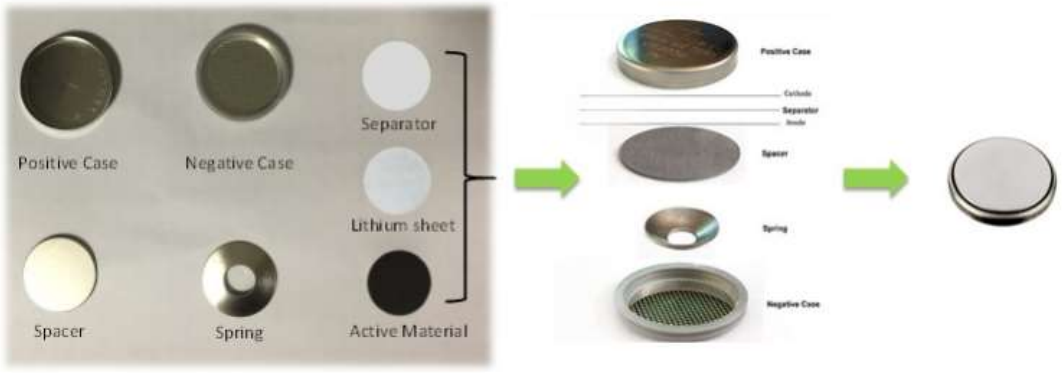

Figure 3.1 Fabrication of the half cells of PDAS-based LIBs and necessary components

The fabrication of PDB LIBs followed the similar process. First, PDB, MWCNT, and PVDF were weighed and mixed in a ratio of 3:5:2. Then, N-Methyl-2-pyrrolidone (NMP) solution was added drop by drop during the mixing process. The mixture was ground in an agate mortar for 30 minutes until a homogeneous slurry was obtained. The slurry was then evenly coated onto aluminum foil, with a loading of 1.2-1.4 grams per square centimeter. The foil was placed in an oven and dried at 80°C for 12 hours. Subsequently, a CR2032 battery was assembled at room temperature using the PDAS method. 1 mol/L (M) lithium bis(trifluoromethanesulfonyl)imide (LiTFSI) in 1,3-dioxolane (DOL) and dimethyl ether (DME) (1/1, v/v) were used as electrolyte, 99.9% lithium foil was used as the anode, and glass fiber was used as the separator. The assembly process of the battery was carried out in an argon-protected glove box, with the water and oxygen content controlled below 1

ppm. Finally, the assembled half-cell was left at room temperature for 24 hours to reach equilibrium before testing its performance. For all-plastic cell, the thoroughly discharged (to 0.005V) half-cell was de-assembled in argon glovebox and the pre-lithiated cathode was applied as anode in the new all-plastic cell, other process was the same as PDB half-cell fabrication.

3.3 Materials Characterization

3.3.1 Scanning Electron Microscopy (SEM)

The morphology characterization of materials through SEM is essentially important to reveal the microstructure features and morphologies of materials. SEM is a useful technique that scans a sample (either organic or inorganic) with high-energy electrons. The electrons interact with the atoms can make the sample to produce signals that contain information about the sample's properties (e.g. size, shape and diameter).

When the electron beam generated by the electron gun bombards the sample, various signals are mainly generated. Secondary electrons can reflect the surface morphology of the sample. However, the yield of secondary electrons does not have a clear dependence on the atomic number, so they cannot be used for compositional analysis. Backscattered electrons can reveal surface morphology and can also be used for qualitative compositional analysis. Transmission electrons can be used for micro-domain composition analysis. The characteristic X-rays can be used to determine the elements present in the micro-regions. Auger Electronics is particularly suitable for surface composition analysis. Fig 3.3 shows the interaction of the electron beam and sample.

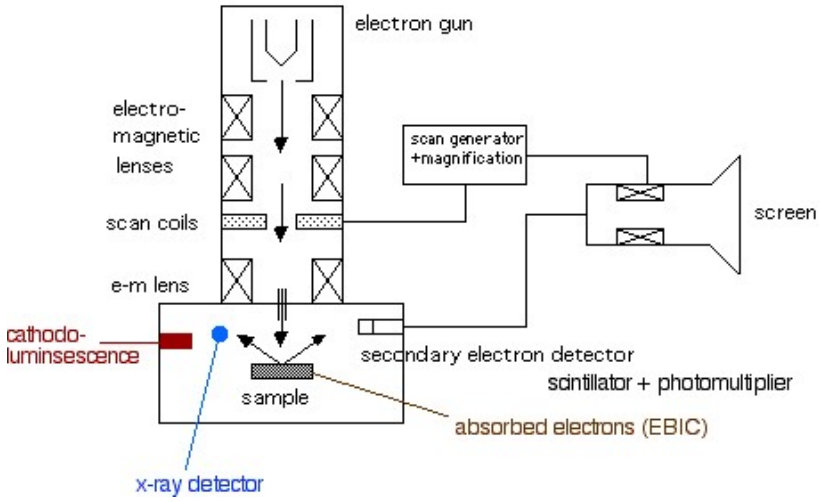

Figure 3.2 SEM structure illustration. Reproduced with permission from [1].

In SEM, the electron beam emitted from the electron gun is focused by electromagnetic lenses into a very small-diameter beam. When the sample is subjected to the electron beam, various signals are generated, and the intensity depends on the surface morphology, composition of the stimulated region, and crystal orientation of the sample. It is important to emphasize that the incident electron beam scans the sample surface point by point, and the image is recorded point by point as well. Therefore, all signals generated from different points on the sample can be recorded, making comprehensive analysis of the sample much more convenient. Fig 3.2 shows the structure of SEM.

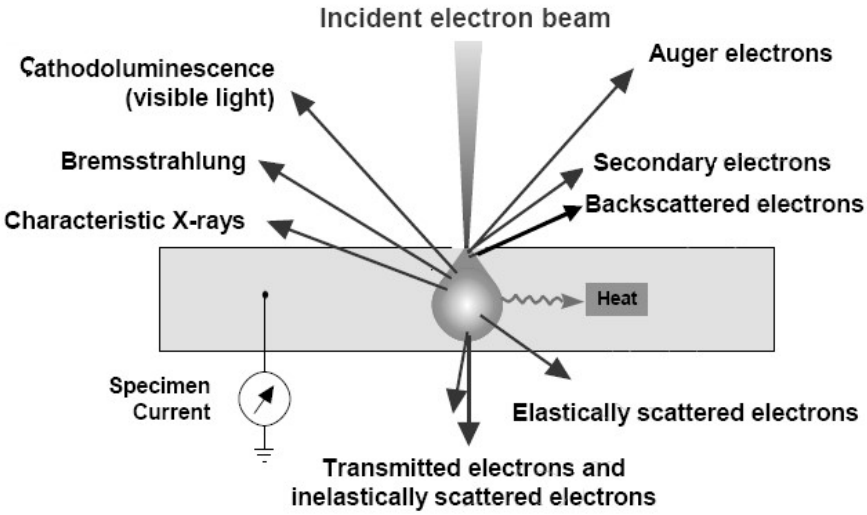

Figure 3.3 Interaction between specimen and electron beam.
Reproduced with permission from [1].

There are two scanning methods for the electron beam on the sample surface. Raster Scanning is used for morphological analysis. Angular Raster Scanning is used for electron channeling pattern analysis.

Fig 3.4 shows the source of SEM filament and the moving path of the ejected electrons by a thermionic electron emission gun. SEM can observe the surface information of a sample in micro world, but the drawback is it can only show a small partial scanning area of the material.

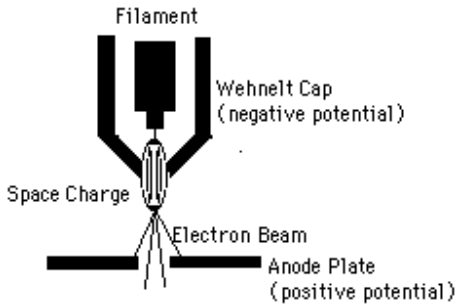

Figure 3.4 Illustration of filament inside the SEM chamber.
Reproduced with permission from [1].

3.3.2 Fourier Transform Infrared Spectra (FTIR)

Fig 3.5 shows a typical FTIR instrument and analysis system.

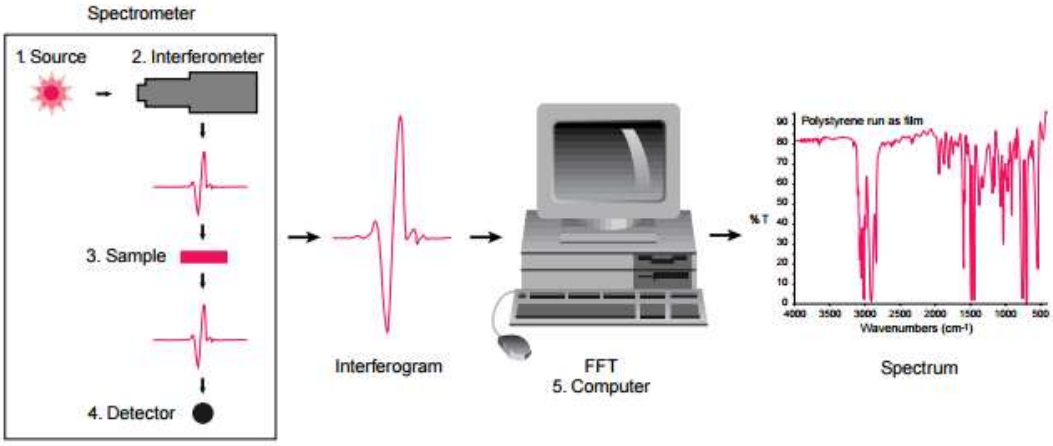

Figure 3.5 FTIR instrumental and data analysis. Reproduced with permission from [2].

Infrared spectroscopy, also known as vibrational-rotational spectroscopy of molecules, is an essential tool for structural analysis of organic compounds. It identifies functional groups in a compound based on the characteristic absorption frequencies of infrared light specific to organic compounds. It can also be used for quantitative analysis by observing changes in the intensity of characteristic peaks.

The radiation energy must have sufficient energy to induce vibrational transitions in the substance. Molecular vibrations must result in a change in the dipole moment. If a vibrational transition does not cause a change in dipole moment, the molecule will not be infrared active. Fig 3.6 shows four typical vibrations of molecules.

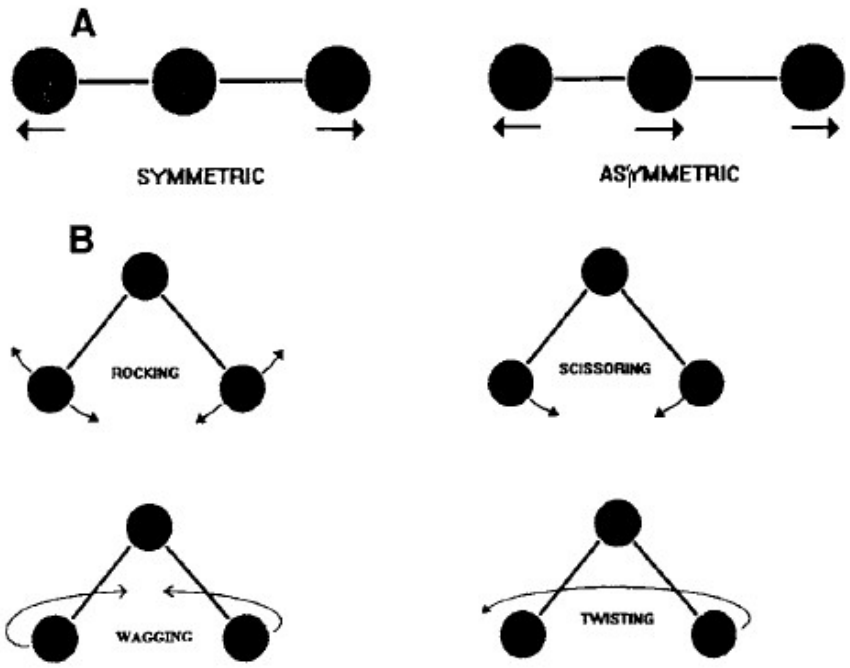

Figure 3.6 Different molecular vibrations. Reproduced with permission from [2].

The vibrations of polyatomic molecules occur in two forms: stretching vibrations and bending vibrations. Bending vibrations appear in the low wavenumber region of the infrared absorption spectrum.

The infrared spectrum obtained after applying Fourier transform to the interferogram of multi-wavelength interference light absorbed by the sample is called FTIR. Since Fourier transform infrared spectrometers can capture all frequency information from the radiation source within any measurement time and eliminate the spectral bandwidth limitations imposed by the slits in dispersive grating instruments, the efficiency of light energy utilization is greatly improved. As a result, FTIR has many advantages, such as shorter measurement time, higher resolution, greater measurement accuracy, reduced stray light, higher sensitivity, and a broader spectral measurement range.

3.3.3 Thermogravimetric Analysis (TGA)

Thermogravimetric analysis (TGA) is a thermal analysis technique that measures the relationship between a substance's weight and temperature or time under a controlled temperature program. The curve obtained from a TGA experiment is known as a thermogravimetric curve. This curve plots mass on the vertical axis, with mass loss indicated from top to bottom, and temperature or time on the horizontal axis. The first derivative of the TG curve with respect to temperature or time yields the first derivative curve (DTG), and the second derivative yields the second derivative curve (DDTG). The first derivative, which represents the rate of mass change, is the most used and is continuously recorded as a function of temperature and time.

TGA is widely used for compositional analysis of samples, stability testing, chemical reaction studies, material quality assessment, and environmental monitoring. Fig 3.7 gives an example of the weight loss of a sample in TGA characterization[6].

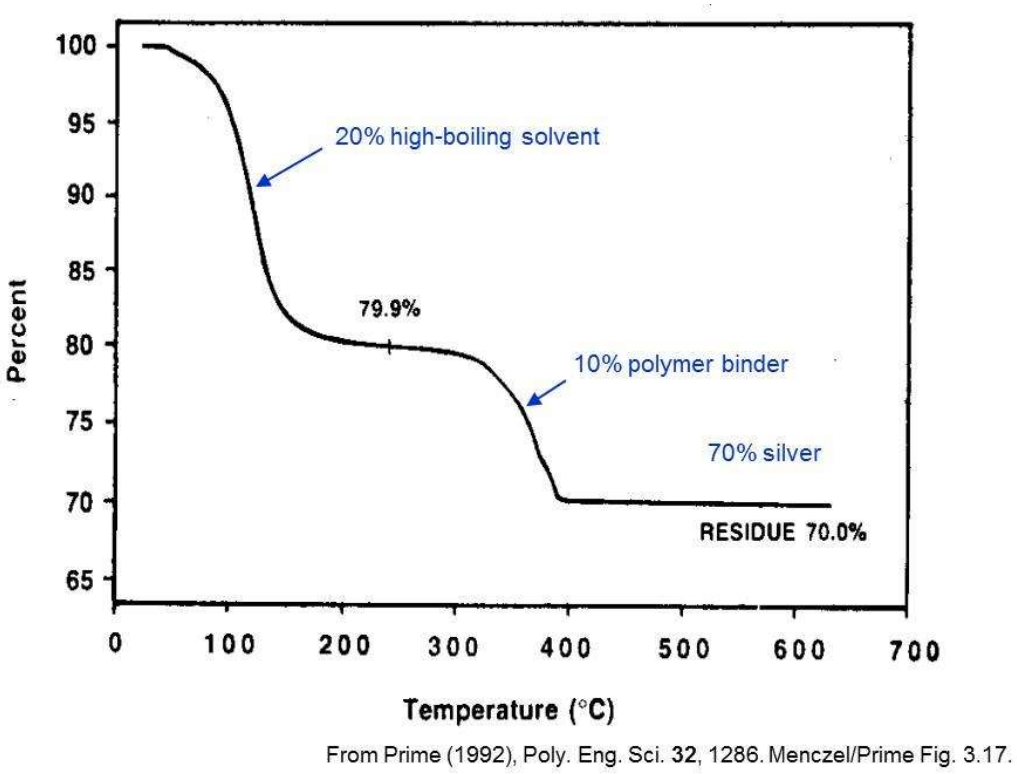

Figure 3.7 An example of TGA curves. Reproduced with permission from [4].

The main working principle of a thermal balance is to combine the circuit and the balance. Through the program temperature controller, the heating electric furnace is heated at a certain heating rate (or constant temperature), when the quality of the tested sample changes, the photoelectric sensor can convert the quality change into a direct current signal. This signal is amplified by the weighing electronic amplifier and fed back to the balance moving coil, generating a reverse electromagnetic torque to drive the balance beam to reset. The potential difference formed by the feedback is proportional to the mass change (that is, it can be transformed into the mass change of the sample). The change information is drawn by a recorder to draw a thermogravimetric analysis (TGA) curve. Fig 3.8 shows the structure of TGA chamber.

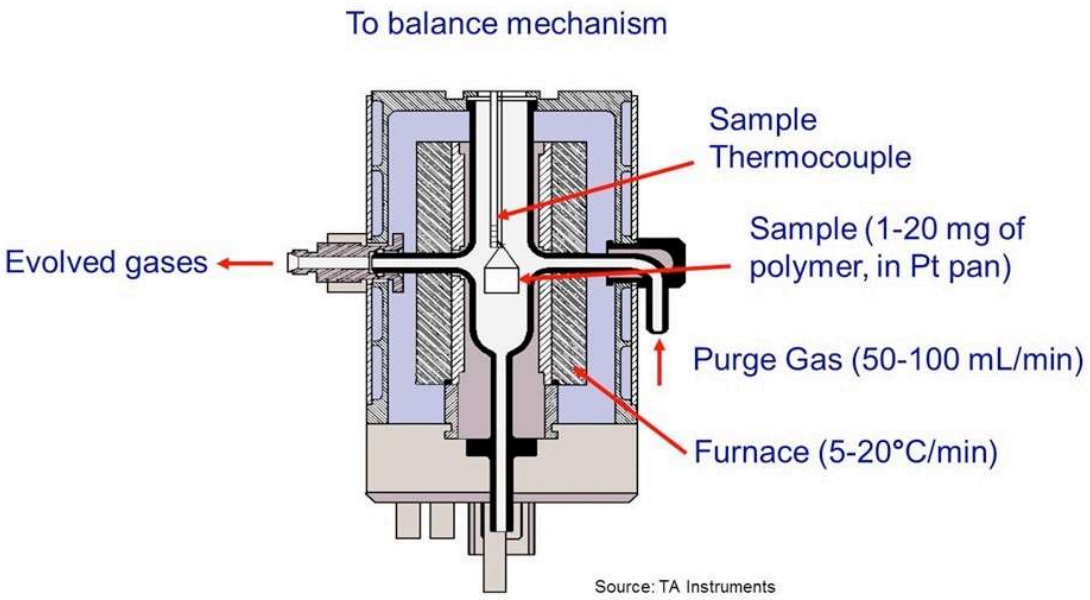

Figure 3.8 Schematic illustration of the physical structure of a typical TGA instrument. Reproduced with permission from [5].

TGA measurement is quite east to conduct, and the process is rapid. Disadvantages contain sensitive environment, which limit the characterization of thermally instable/volatile materials.

3.3.4 X-ray Diffraction (XRD)

When the scattered X-ray and the incident X-ray have the same wavelength, it will cause diffraction to the crystal, that is, when the optical path difference caused by the interplanar spacing is equal to an integer multiple of the wavelength. Comparing the unique diffraction pattern of each crystal substance with the standard diffraction pattern, using the principle of three peaks, the phases existing in the sample can be identified.

For diffraction to occur, the Bragg formula must be satisfied: $2d\sin\theta=n\lambda$ (d: interplanar spacing; θ: Bragg angle; λ: X-ray wavelength; n: reflection order). When X-rays are irradiated to the sample, the scattered X-rays of each atom in the crystal will interfere, and strong X-ray diffraction lines will be generated in a specific direction. When X-rays irradiate the sample from different angles, they will be diffracted on different crystal planes. The detector will receive the number of diffracted photons reflected from the crystal plane to obtain a spectrum of the relationship between angle and intensity. Fig 3.9 demonstrates diffraction that satisfy the Bragg equation.

The generation of X-rays is produced by the accelerated electron flow of 30-60KV in the X-ray tube (vacuum 10^{-4}Pa), impacting the target surface of metal (such as pure Cu or Mo). Commonly used rays are MoKα rays, including Kα1 and Kα2 rays (intensity 2:1), with a wavelength of 71.073pm.

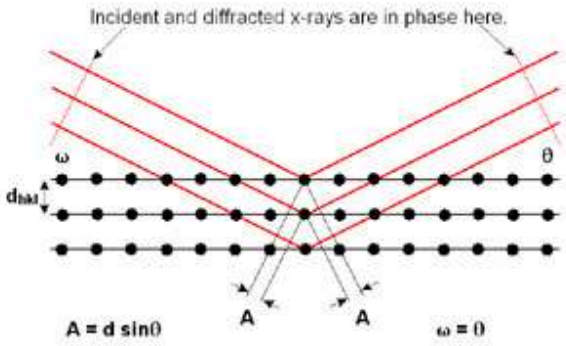

Figure 3.9 Diffraction of X-rays through lattices. Reproduced with permission from [7].

XRD can be used to gather information of crystal structure and quantitative parameters of the lattice, which offers a powerful tool to determine an unknown crystalline material. However, its characteristics limit the characterization of amorphous materials and samples with low crystallinity.

3.3.5 ^{1}H-Nuclear Magnetic Resonance (NMR) and ^{13}C-NMR

When the rotation of the charged nucleus placed in a strong magnetic field, it must be rearranged along the direction of the magnetic field. When the spin axis is deviated from the direction of the applied magnetic field, the magnetic field generated by the nuclear spin will interact with the external magnetic field, causing the nucleus to swing around the original axis along the conical side in addition to the spin, this type of motion is called precession. At this time, if there is a radio frequency field with a frequency equal to the precession frequency, the atomic nucleus will resonate with it and absorb energy to make the nucleus transition to a higher energy state. This phenomenon is nuclear magnetic resonance. Since different nuclei resonate at different frequencies, these differences can be used to identify various elements and isotopes. It should be noted here that the high-energy state of the nucleus will return to the low-energy state through the relaxation process, so that a stable signal of the resonance absorption peak can be maintained.

In practice, hydrogen nuclei are influenced by the surrounding constantly moving electrons. In various organic compounds, the density of the electron cloud around each hydrogen nucleus differs, leading to variations in resonance frequencies. The displacement of resonance absorption peaks caused by these differences is known as chemical shift, with tetramethylsilane (TMS) used as the reference standard. The splitting of absorption peaks is due to spin-spin coupling, resulting in the splitting of spectral lines.

Compared to proton NMR[8], ^{13}C-NMR[9] is more challenging to detect due to its natural abundance of only 1% and a magnetic moment that is only a quarter of hydrogen atoms. Despite these challenges, carbon NMR offers several advantages. It provides detailed

information about the molecular backbone, with a wide range of chemical shifts and low coupling probabilities between carbon atoms, which can be decoupled to simplify the spectrum. Additionally, when carbon atoms are bonded to electronegative groups, the chemical shift moves downfield. Fig. 3.10 shows the structure of NMR.

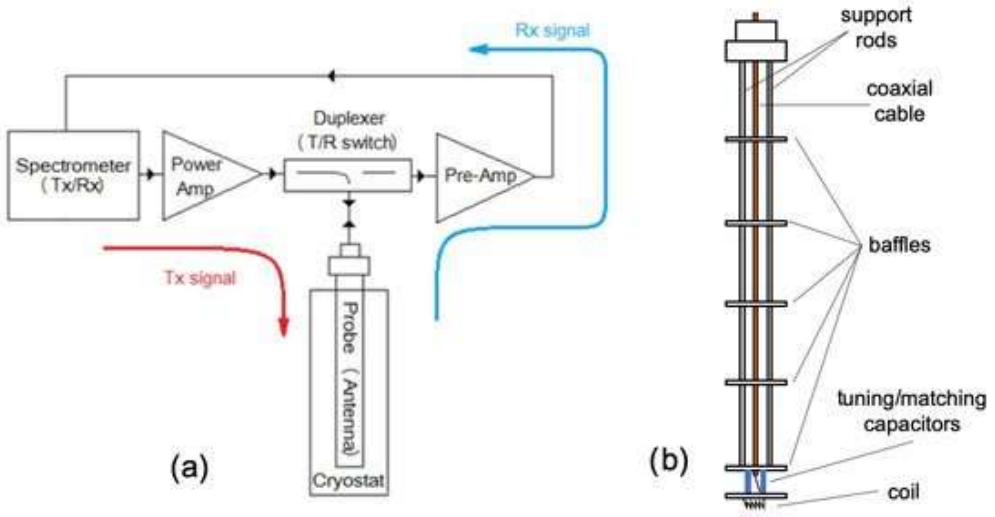

Figure 3.10 a) Illustration of the structure of NMR. b) Injection chamber of NMR to insert samples. Reproduced with permission from [8].

3.3.6 Elemental Analysis (EA)

Elemental quantitative analysis is a technique used to determine the content of elements within organic compounds and analyze the composition of these compounds. Typically, elemental quantitative analysis focuses on common elements found in organic compounds, such as carbon, hydrogen, oxygen, sulfur, phosphorus, and halogens. The percentage of oxygen is calculated by subtracting the measured values of other elements from 100%.

The process of determining the elements in an organic compound generally involves three steps: decomposition of the sample, elimination of interfering elements, and measurement of the elemental content in the decomposition products. The decomposition products can be measured using chemical analysis or physical and physicochemical analysis methods. Depending on the chosen measurement method, it may be necessary to eliminate

interfering elements from the decomposition products before measurement. The combustion process usually takes more than 30 minutes. Common interfering elements include nitrogen, sulfur, and halogens. The thermal decomposition products of silver permanganate are generally used to eliminate these interferences. During the combustion of nitrogen-containing compounds, nitrogen dioxide is produced, which can be absorbed by activated manganese dioxide. Finally, the various elements are quantitatively measured using absorbents or titrants. Fig 3.11 shows the workflow of a typical EA experiment.

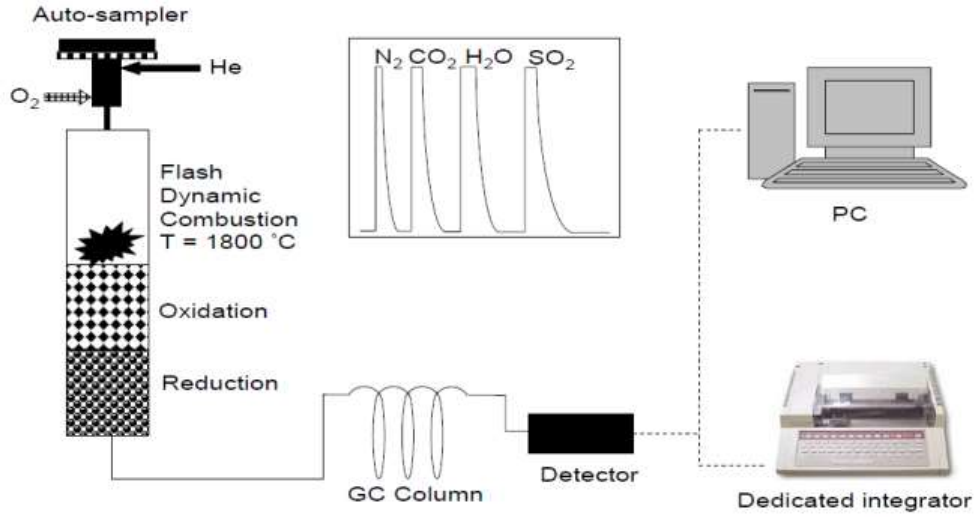

Figure 3.11 Illustration of the EA instrument. Reproduced with permission from [9].

3.3.7 Energy-Dispersive X-Ray Spectroscopy (EDS) Elemental Mapping

EDS can be combined with SEM, TEM, and other instruments, with the SEM-EDS combination being the most widely used microscopic analysis tool. The development of EDS has made it almost a standard feature of SEM, serving as a primary method for micro-area composition analysis. EDS can quickly and simultaneously conduct qualitative and quantitative analysis of all elements from Be to U in the micro-areas of various samples, often completing the analysis in just a few minutes. The geometrical requirements for the position between the sample and the detector are low, allowing X-ray scanning and surface distribution results to be obtained at low magnification. EDS requires a low probe current, causing minimal damage to samples sensitive to electron beam irradiation, such as biological samples, fast ion conductors, and glass. The detection limit generally ranges

from 0.1% to 0.5%, with the quantitative relative error for main elements with medium atomic numbers and no overlapping peaks being about 2%.

The principle is that the intensity of the characteristic X-rays of a specific element in the sample is proportional to the content of that element in the sample. Therefore, by measuring the X-ray intensity of the element in the sample and comparing it to the intensity in the standard under the same conditions, an approximate concentration ratio can be determined. When the elements and contents of the sample and standard are similar, this ratio generally holds, though corrections are often necessary to obtain accurate concentrations. Standardless quantitative analysis is a rapid method of X-ray microanalysis, relying on pure physical calculations or a database of standards applicable to different experimental conditions. Its accuracy is lower than that of standard-based quantitative analysis.

There are three commonly used scanning methods of EDS analysis. Point Analysis is highly accurate and is used for compositional analysis of microstructures with low element content. Line Scan Analysis can obtain the distribution of elements in different phases or regions can be visually observed. Surface Distribution is commonly used to study the distribution of impurities, phases, and element segregation in materials, often in conjunction with morphological analysis.

3.3.8 Galvanostatic Charge-Discharge

The constant current charging and discharging method is a battery charging and discharging technology that effectively controls the battery’s charging and discharging process to enhance its lifespan and performance. The principle of constant current charging and discharging is to input a fixed current into the battery during charging, maintaining the battery’s voltage at a certain level to achieve charging. During discharging, a fixed current is drawn from the battery, maintaining the battery’s voltage at a certain level to achieve discharging. Main advantages including effective control, this method effectively manages the charging and discharging process, improving the battery's lifespan and performance. Also, it can help reduce the battery temperature, which slows down battery aging. However,

this method is time-consuming, the charging and discharging process takes a longer time, making it unsuitable for applications requiring rapid charging and discharging.

Galvanostatic charge and discharge method can also be applied to study electrochemical reaction kinetics and material electrochemical performance. By recording the battery's voltage and current curves, various electrochemical performance parameters, such as battery capacity, internal resistance, and polarization, can be obtained. Thus, it is widely used in battery research to study the performance and characteristics of new battery materials. It can also assess the performance of power sources and analyzing and optimizing energy storage systems. During constant current charging and discharging experiments, appropriate constant current values, charging and discharging conditions, and battery storage condition can be tuned.

3.3.9 Cyclic Voltammetry (CV)

Cyclic voltammetry is an analytical method based on the current-voltage curve obtained by scanning the potential from a starting value to a final value and then reversing the scan back to the original starting potential. The relationship between the potential and scan time creates a triangular waveform. If the first half of the scan (rising voltage) represents the cathodic process where the depolarizer is reduced on the electrode, then the second half of the scan (falling voltage) represents the anodic process where the reduction product is reoxidized. One triangular waveform scan completes a cycle of reduction and oxidation processes, hence the term cyclic voltammetry.

If the electrode process is reversible and the reaction products are stable, cyclic voltammetry is a convenient method for determining the standard electrode potential. This technique not only helps to identify and characterize intermediate products of electrochemical processes but also provides information about their electrochemical and other properties. Cyclic voltammetry can also be used to identify products of electrochemical-chemical coupling reactions.

3.4 Overview of Methodologies

Various characterization methods were used in the study to obtain different information about the synthesized samples. SEM was used to obtain information about the morphology and surface of the materials. XRD provided information on the crystal structure. NMR was used to confirm the successful synthesis of polymers and the presence of functional groups. FTIR was used to obtain information on the material's skeletal structure, functional groups, and changes in the valence state of active sites during charge-discharge processes. EA and EDS provided information on the overall and the specific area of elemental composition. CV and galvanostatic charge-discharge methods were used to obtain important parameters related to battery performance.

References

[1] Q. Cao, C. Yu, X.-F. Cheng, W.-J. Sun, J.-H. He, N.-J. Li, H. Li, D.-Y. Chen, Q.-F. Xu, and J.-M. Lu. *Sensors and Actuators B: Chemical*. **2020**, 320, 128390.

[2] P. Kolar, M. S. Grbić, and S. Hrabar. *Sensors*. **2019**, 19, 3064.

[3] J. Goldstein. *Springer Science & Business Media.* **2012**.

[4] J. I. Goldstein, D. E. Newbury, J. R. Michael, N. W. Ritchie, H. J. Scott, and D. C. Joy. *Springer.* **2017**.

[5] P. R. Griffiths, J. A. De Haseth. *Fourier Transform Infrared Spectrometry*. **2007**, 171.

[6] A. Coats, J. Redfern. *Analyst.* **1963**, 88 (1053), 906-924

[7] M. von Laue. *Eine Quantitative Prüfung der Theorie für die Interferenz-erscheinungenbei Röntgenstrahlen*. **1912**.

[8] B. E. Mann. *Elsevier.* **1974**, 12, 135-213.

[9] Kalinowski, H.-O. Berger, and S. Braun. *Carbon-13 NMR Spectroscopy*. **1988**.

Chapter 4

Novel Ion-in-conjugation Polymers as Promising Cathode Electrodes for Lithium-ion Organic Batteries

Ion-in conjugation polymer is a kind of polymer that has ion fragments in polymer chains. Inspired by the high conductivity, simple chemical structure and multi active sites (carbonyl groups) to store lithium ions, two kinds of ion-in-conjugation polymer 1,5-PDAS and 2,6-PDAS are synthesized as promising cathode materials in LIBs. Characterization methods like SEM and FTIR are applied to obtain information of the morphology and chemical structure of these polymers. Electrochemical experiments show that these polymers have decent performance as LIB cathodes.

4.1 Introduction

Inspired from their good conductivity and multi active functional groups with simple synthesis, ion-in-conjugation polymer have gained interest as a promising conjugated polymers for LIBs. The existing ion-in-conjugation polymers consist of three types: d-π conjugation polymers, polysquaraines, and polysquaramides. Finally, we chose polysquaramides as the polymer for electrode materials because they exhibit the best conjugation.

In this chapter, two kinds of ion-in-conjugation polymers have been synthesized. Characterization and battery performance show the polymers 1,5-PDAS and 2.6-PDAS are decent to be applied as cathode materials for LIBs. The two regioisomers also provide a good perspective to investigate the influence of functional groups at different location. Result from XRD shows the information of crystallinity, which is directly revealed by the absorption curves and may lead to the different electrochemical performance especially at the first three cycles in battery test. Battery tests showed that both polymers exhibit good electrochemical performance. Among them, 1,5-PDAS has a higher capacity but lower stability, while 2,6-PDAS demonstrates excellent cycle stability but with a relatively lower capacity. Despite their mediocre performance under high-rate charge and discharge conditions, both polymers outperform other conjugated polymers in terms of overall performance. The successful synthesis of the ion-in-conjugation polymer provides new strategy for future electrode material design.

4.2 Synthesis and Electrochemical Test

4.2.1 Synthesis of 1,5-PDAS and 2,6-PDAS

The preparation of 1,5-PDAS: Firstly, 1,5-diaminoanthraquinone (1, 5-DAAQ) is added into a flask, then added with squaric acid (SA) and dissolve the ingredients with butyl ethanol (n-BuOH). Both DAAQ and SA are weighed 2 mmol, 476.5mg for DAAQ and 228.1mg for SA, together with 50 mL of BuOH and mix them to fully dissolve the organic

powder. The complex was stirred and refluxed with a temperature of 120-150 °C for one day. Then the complex was filtered and washed by DI water (deionized H_2O), the filter tablet will also be cleaned by an extractor. The filter is then washed by tetrahydrofuran for 24h. At last, the filtered complex was placed under vacuum and corresponding sample was obtained. Poly (2, 6-diaminoanthraquinone-squarine) (2, 6-PDAS) was prepared followed the same process. 2,6-PDAS exhibit as dark red powder while 1,5-PDAS have dark color. Fig 4.1 illustrates synthesis of 1,5-PDAS and 2,6-PDAS, respectively.

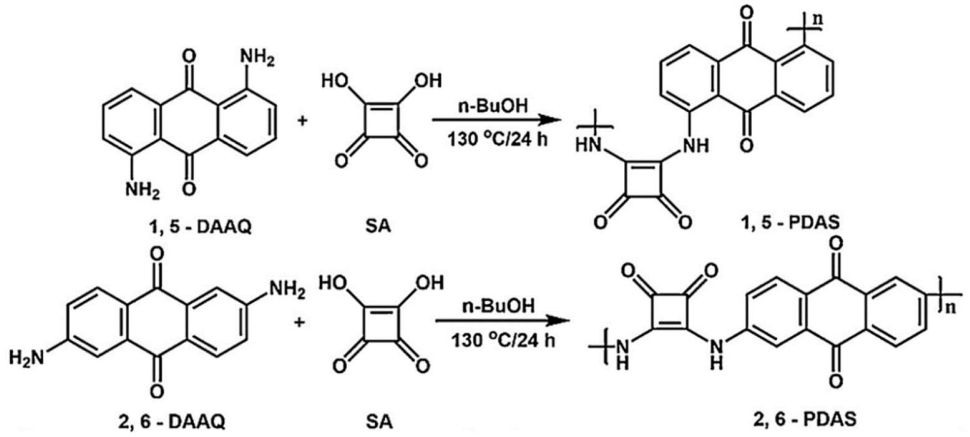

Figure 4.1 Synthesis route of 1,5-PDAS and 2,6-PDAS

4.2.2 Electrochemical Measurements of PDAS

The assembled coin cells were tested by NEWARE multifunctional battery test systems with galvanostatic charge-discharge in the scope from 1.4 to 3.5 V. Charge and discharge curves, cycling stability, rate performances and long-term cycling results can be obtained. Cyclic voltammetry (CV) parameters are set between 3.5-1.4 V at a scan rate of 0.1 mV/s via battery CV testing system CV view2 software.

4.3 Results and Discussions

SEM image of the 1,5-PDAS and 2,6-PDAS directly shows the difference of morphology of the two polymers. Fig 4.2a shows 1,5-PDAS have long, rod-like

granules with smooth surface the particle size is around 1-2 μm. 2,6-PDAS have different porous structure and twist with each other to form an amorphous polymer as shown in Fig 4.2b, which suggests it has lower crystallinity.

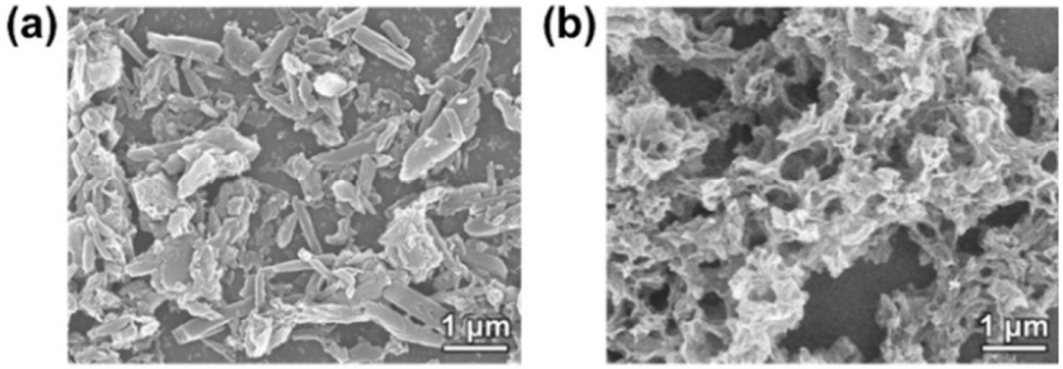

Figure 4.2 SEM image of two polymers. a) 1,5-PDAS; b) 2,6-PDAS

Fig 4.3 shows the XRD patterns illustrate both 1,5-PDAS and 2,6-PDAS have an absorption peak at 26°, which is due to the π-π staking of the conjugated structures[1-2]. 1,5-PDAS also have a strong peak at 8°, but it is almost impossible to figure out the exact stacking of the lattice and which lattice plane it comes from due to the complicated staking of the polymer chains. In addition, it is too intricate to fit the model of the polymers as they do not behave like 2D COFs (covalent organic framework) with regular planar structure.

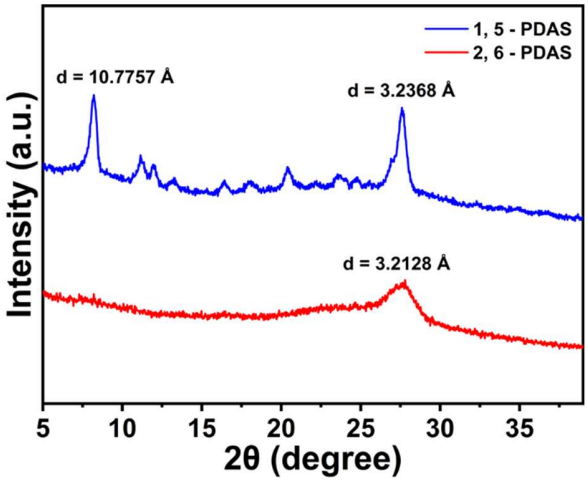

Figure 4.3 XRD pattern of 1,5-PDAS (blue line) and 2,6-PDAS (red line)

From FTIR spectra, PDAS polymers are synthesized successfully. As shown in Fig. 4.4, the stretch vibration of N-H groups in 1,5-DAAQ at 3419cm^{-1} and 3313 cm^{-1} as well as the vibration of hydroxyl group at 3502 cm^{-1} disappeared in PDAS polymers, which indicates the combination of -NH_2 and -OH groups. The two absorption peaks of carbonyl groups at 1797 and 1720 cm^{-1} indicates the condensation reaction happens in ortho-position[3-4]. The similar spectrum of 2,6-PDAS demonstrates 2,6-DAAQ and SA also condensed into polymer successfully in ortho-position.

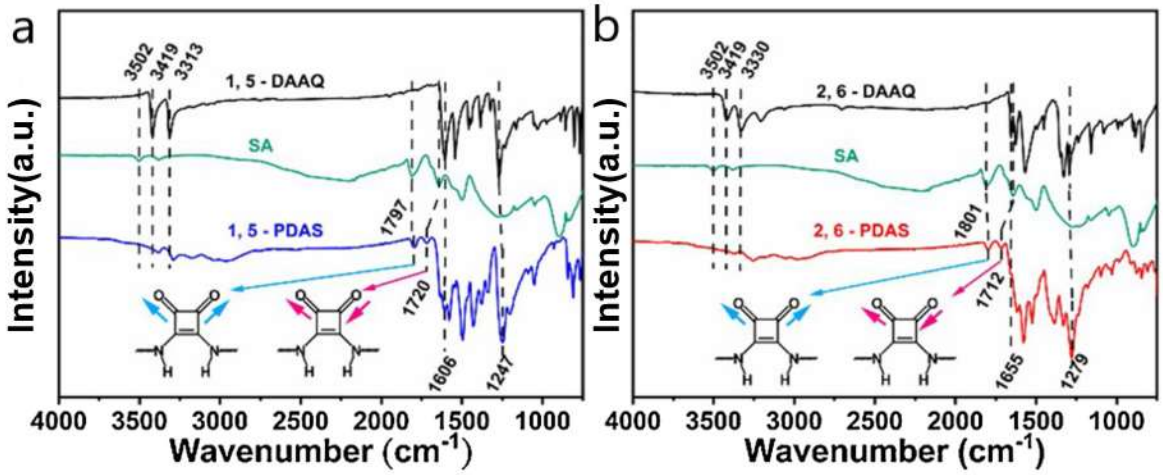

Figure 4.4 FTIR spectra of 1,5-PDAS (a) and 2,6-PDAS (b)

The thermogravimetric analysis is applied to characterize the thermal stability of the two polymers. Fig. 4.5 illustrates both 1,5-PDAS and 2,6-PDAS have decent thermal stability, which is important to be applied as electrode materials in LIBs considering the working environment (at least work during -20℃~60℃). Both polymers can endure temperature beyond 200℃. 1,5-PDAS have better thermal stability and only loses 5% of initial weight until 285℃, while 2,6-PDAS loses 5% of its weight at 209℃ as shown in Fig. 4.5.

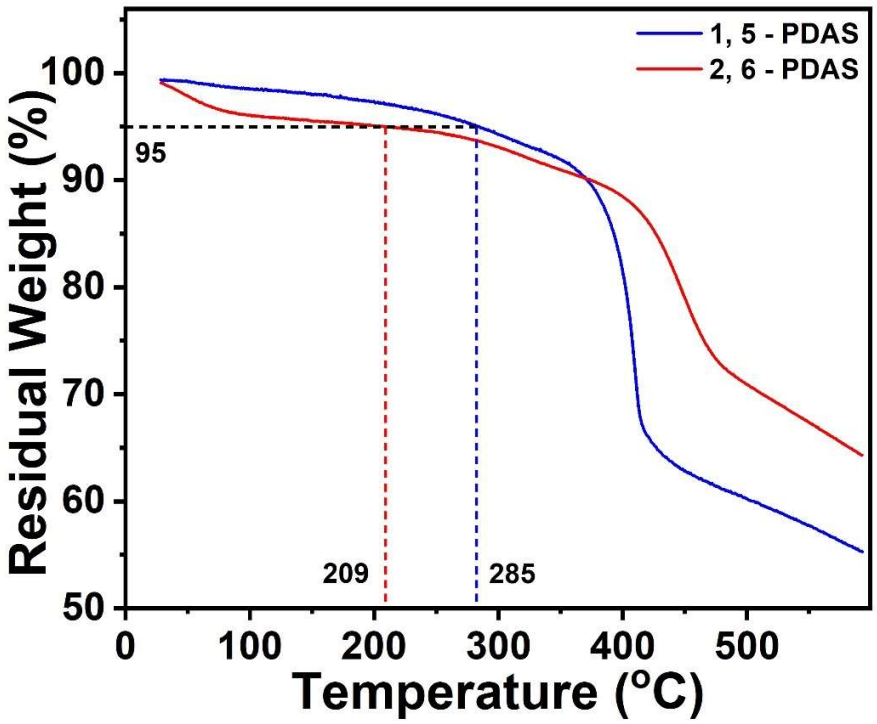

Figure 4.5 Weight loss of PDAS during temperature rising in thermogravimetric analysis

Diagrams from ^{13}C-NMR further affirm the backbone carbon chain of the two polymers to ensure their condensation. As shown in Fig. 4.6, carbon atoms adjacent to oxygen g and i have the highest chemical shifts due to the strong electronegativity of oxygen atoms, thus have strong shield effect in magnetic field, h belongs to the carbon atoms on SA C=C bonds. Peaks a-f belong to the carton atoms in aromatic C6 rings. Peak d is difficult to identify due to spin-spin coupling and splitting caused by electrons.

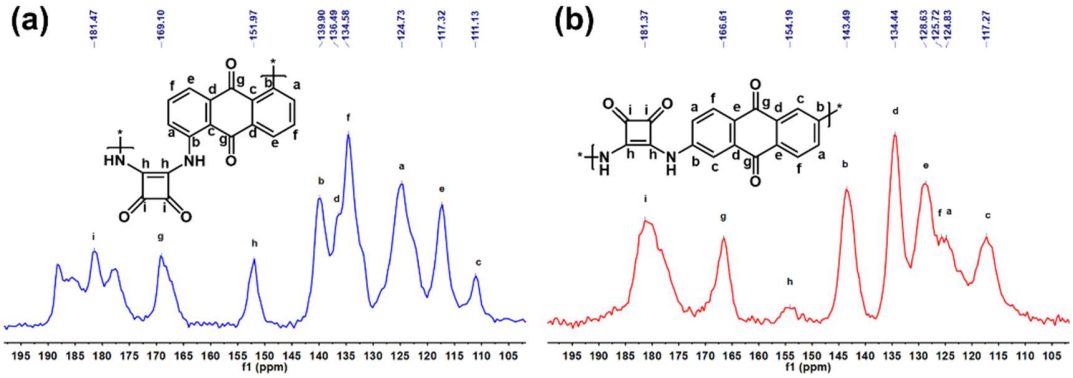

Figure 4.6 Spectra of 1,5-PDAS and 2,6-PDAS under solid-state ^{13}C-NMR

After success synthesis and characterization of the PDAS polymers, their electrochemical performance has been investigated as cathode materials. Neware battery testing station is used to test different function of the fabricated half-cells.

The galvanostatic process is first investigated at the constant current density of 100 mAh/g during charge and discharge process. As shown in Fig. 4.7, 1,5-PDAS and 2,6-PDAS almost have the same performance during galvanostatic process. Both materials have a plateau at about 1.6-2.2V during discharge process, which is due to the absorption of lithium ions of carbonyl groups. The reversible delthiation process also happens during recharge process at the plateau at about 1.8-2.6V. 1,5-PDAS also be found have much higher initial specific capacity at the first cycle and soon attenuate into normal 200 mAh/g energy density. This is partly because of the formation of solid electrolyte surface (SEI) as PDAS have a moderate low potential as cathode materials[5-6].

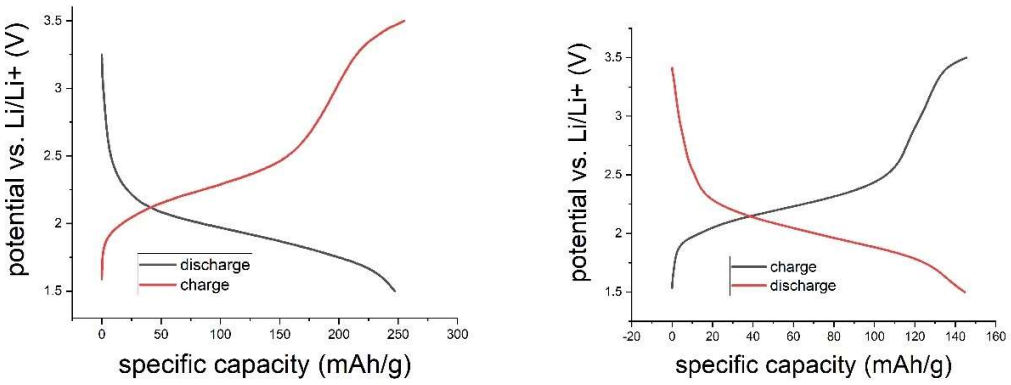

Figure 4.7 Profiles of 1,5-PDAS (left) and 2,6-PDAS (right) during charge and discharge process at the initial cycle

Fig. 4.8 shows the CV curves of 1,5-PDAS and 2.6-PDAS of the initial three recycles from 1.2-3.5V, with a swap current at 0.1 mV/s. In the first cycle, both PDAS exhibit four peaks during anodic scan at around 2.5V, this is a typical oxidation process of carbonyl groups in enolation. The first peak appears at the 2.51 V, oxidation peak of carbonyl group also appears in the same potential for the last two cycles, indicating the polymer is stable. The first carbonyl group is elongated by lithium ion at 2.51 V and here rises an oxidation peak, the other three carbonyl groups also lead to three small peaks when lithiated at 2.63, 2.67, 2.71 V discovered in 1,5-PDAS. In 2nd and 3rd cycles four pairs of peaks are expected to see corresponding to the four redox centers of carbonyl groups, but clearly distinguished pairs of redox peaks are disappeared because of the fast transformation between the radical anion and dianion, which has also been observed on other polysquaraines and polysquaramides[7]. However, 2,6-PDAS does not have these four peaks at initial oxidation cycle. Hypothesis have been proposed that the high crystallinity of 1,5-PDAS and its bigger spatial impulsion of carbonyl groups interfere the transformation of lithium ions among molecules, so it exhibits four oxidation peaks while for amorphous porous 2,6-PDAS there is no such considerable hinderance, so the peaks integrate into one peak. In addition, after saturated lithiation and totally be oxidized during the anodic scan of 1st cycle, 1,5-PDAS can also transfer ions inside the polymer chains, so 2nd and 3rd cycles also have an integrated peak. The 2nd and 3rd cycle have high similarity and well symmetry which indicates the two polymers are stable and highly reversible in redox reaction.

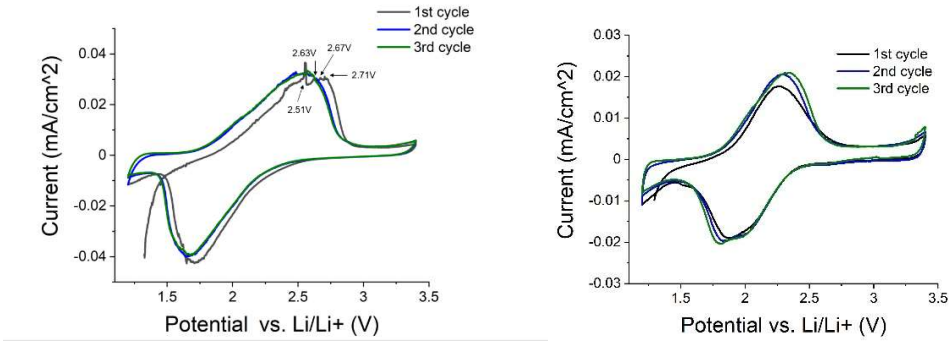

Figure 4.8 CV curves of 1,5-PDAS (left) and 2,6-PDAS (right)

Fig 4.9 shows the rate capacity of 1,5-PDAS and 2,6-PDAS to further determine their potential as cathode materials. 1,5-PDAS have higher initial specific capacity at around 280 mAh/g at 20 mA/g but with poor endurance of higher current density, the capacity will largely decrease when current density is beyond 500 mA/g, only 1/6 of the capacity is maintained comparing 1,5-PDAS under 20mA/g and 1500 mA/g current density. 2,6-PDAS have better stability to maintain its performance under large current density, it can still reserve 40% of the capacity at 1500 mA/g comparing to 20 mA/g current density. Rate performance exhibit PDAS are not good materials for fast-charging materials.

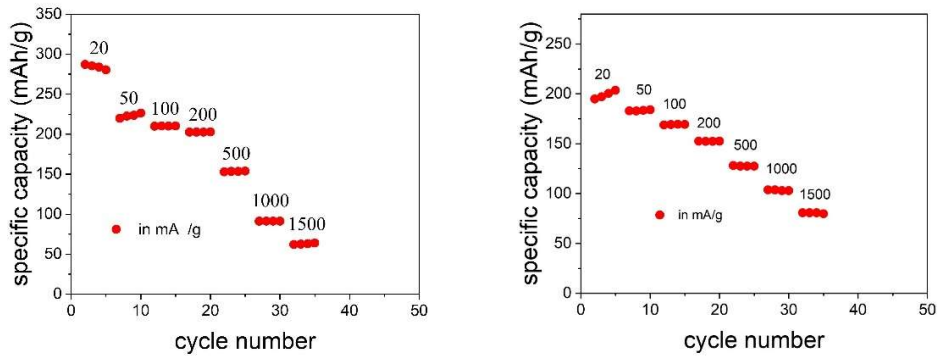

Figure 4.9 Rate capacity of 1,5-PDAS and 2,6-PDAS under 100 cycles at current density of 20~1500 mA/g

Fig 4.10 illustrates PDAS polymers as excellent stable organic cathodes after cyclic test for 100 recycles with current density of 100 mA/g. 1,5-PDAS again shows its better

specific capacity at 250 mA/g but will gradually decay into 200 mA/g, after 100 cycles 80% of the energy density is maintained. 2,6-PDAS exhibit more excellent stability than its isotope, it almost never decays after 100 recycles and amazing 98% energy retention is achieved after 100 cycles. 2,6-PDAS have almost 100% Coulombic efficiency which indicates it is perfectly reversible, however, the drawback is at the cost of capacity, its specific capacity is always lower than 1,5-PDAS.

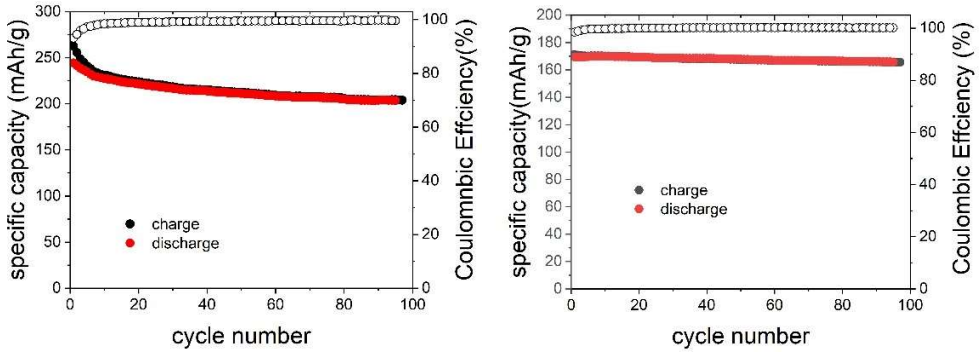

Figure 4.10 Cycling performance of 1,5-PDAS and 2.6-PDAS with 100 cycles

In the first part of the experiment, a novel ion-in-conjugation polymer and its isomers were successfully synthesized through a one-step condensation reaction. Compared to other organic materials, these two polymers, 1,5-PDAS and 2,6-PDAS, exhibit certain advantages as high-quality organic cathode materials. Additionally, this study delves into comparing the different functional group positions and explores how they influence the electrochemical performance of the materials, thus providing insights for designing new organic electrode materials with higher energy density and stability.

The successful fabrication of the batteries demonstrated that all four carbonyl groups in PDAS can absorb lithium ions, resulting in a high capacity. In previous literature reviews, most polymers or conjugated molecules with more than two carbonyl groups often led to significant carbonyl deactivation. Therefore, the proposed discharge/charge mechanism of PDAS is a reversible four-electron reaction (for each monomer). The theoretical capacity of PDAS is 439 mAh/g, with 1,5-PDAS achieving 250 mAh/g and 2,6-PDAS achieving 170 mAh/g, both being reversible. This suggests that the carbonyl groups on the four-

membered ring can also exhibit electrochemical performance, which could be a focus of future studies, as they offer higher specific capacity compared to six-membered rings.

1,5-PDAS exhibits higher energy density, and in half-cell studies, it can even reach a specific capacity of 450 mAh/g in the initial cycle, but this quickly decays, indicating that irreversible lithium-ion insertion occurs during the first cycle, forming a stable structure. Additionally, during CV testing, the cathodic scan during the first cycle shows a large current at 1.2 V, and this process is irreversible, further supporting the occurrence of an irreversible reaction during the first discharge. This suggests that 1,5-PDAS undergoes a different discharge process compared to 2,6-PDAS. It is likely that the anthraquinone structure absorbs lithium ions, forming a LiC6 complex, and these reactions are irreversible, leading to a low Initial Coulombic Efficiency (ICE), typically below 50%. This explains the experimental phenomenon where 1,5-PDAS shows a high capacity during the first few cycles but rapidly declines.

The differences between 1,5-PDAS and 2,6-PDAS highlight the importance of morphology in electrode materials. XRD combined with SEM clearly shows that 2,6-PDAS has greater crystallinity compared to 1,5-PDAS, and its structure is more stable. This may explain why 2,6-PDAS exhibits much better cycling performance than 1,5-PDAS. Experiments also demonstrate that CNTs enhance the performance of organic electrodes more effectively than traditional carbon black, validating the advantage of using nanotechnology to tune electrochemical properties. Nanostructures can provide a larger surface area, facilitating easier lithium-ion diffusion.

Despite the many advantages of 1,5-PDAS and 2,6-PDAS, they share a common issue: the low voltage platform results in a specific energy density that is not ideal compared to traditional inorganic materials. The degradation of 1,5-PDAS also limits its application in LIBs, as the irreversible reactions during the first cycle can damage the battery and even pose safety concerns. Future research should focus on increasing the voltage of organic materials as cathodes or using them as both cathodes and anodes in all-plastic batteries. Building on this, methods like nanotechnology could be used to prepare nanoparticles of

these polymers, increasing their surface area and making lithium-ion conversion easier and faster, thereby improving their performance.

4.4 Conclusions

In conclusion, a novel squirimide polymer with its regioisomer is synthesized successfully through condensation reaction of DAAQ and SA through one step. These polymers 1,5-PDAS and 2,6-PDAS both have some advantages as decent organic cathode materials comparing with other organic materials. In addition, these polymers give researchers a deep understanding of different location of the functional groups and investigate how they influence the electrochemical performance of the materials to provide ideas to design novel organic electrode materials with higher energy density and stability. It is optimistic to predict after the continuous effort of the researchers, organic LIBs will become commercial in the future to replace the expensive and toxic inorganic LIBs.

Battery test successfully proves all the four carbonyl groups in PDAS can absorb lithium ions and have large capacity. In previous literature review, most polymers or conjugated molecules with more than two carbonyl groups will lead to the serious deactivation of the carbonyl groups. Fig 4.11 demonstrates the proposed discharge/charge mechanism of 1,5 and 2,6-PDAS. The theoretical capacity of PDAS is 439 mAh/g, 250 mAh/g of 1,5-PDAS and 170 mAh/g of 2.6-PDAS are fabricated and reversible. This reveals the carbonyl groups on four membered rings can exhibit electrochemical performance and latter research could consider these structure as they have higher specific capacity than six membered rings.

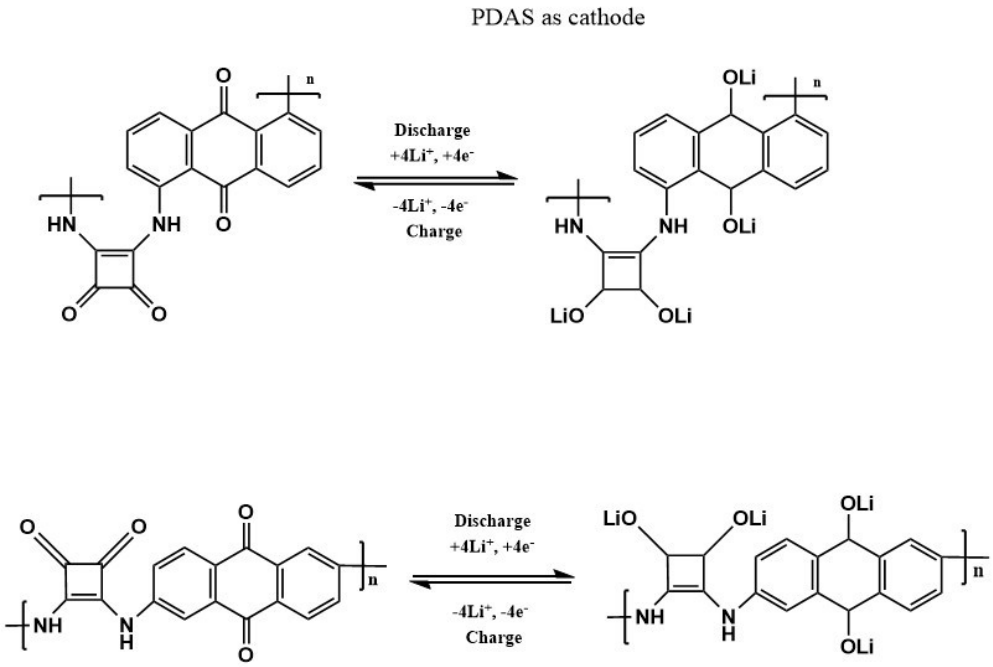

Figure 4.11 Mechanism of 1,5-PDAS and 2.6-PDAS during discharge and recharge process

1,5-PDAS have higher energy density and in the investigation of the half-cells, it can even reach the specific capacity of 450 mAh/g at the initial cycle but will soon decay. Also, in CV test, during the 1st cycle cathodic scan diagram shows a large current will arise during the 1.2 V and this process is not reversible as latter cycles will not have this pattern, which indicates 1,5-PDAS have different discharge process compared to 2,6-PDAS. This is probably because it forms a SEI (solid electrolyte interphase) and the AQ structure could also absorb lithium ions to form LiC6 complex and these reactions are irreversible as the Coulombic efficiency is at very low level, usually lower than 50%. This explains the capacity is quite high at the initial several cycles of 1,5-PDAS and will soon decrease.

The difference of 1,5 and 2,6-PDAS indicates that morphology is of great significance of the electrode material. Experiment proves that CNT will largely enhance the performance of organic electrodes than conventional carbon black (batteries with carbon black show little specific capacity compared to MWCNT), which verifies the advantage of using nanotechnology to tune the electrochemical properties. Nanostructure can offer larger surface area and easier for lithium-ion diffusion.

Although 1,5-PDAS and 2.6-PDAS have many advantages, they have a common problem: the specific energy density of the material is not pleasant comparing with inorganic conventional materials as a result of low potential platform. The decay of 1,5-PDAS also limit its application in LIBs as irreversible reaction during the first cycle will harm the cell and may even cause safety issues. Future research should focus on (1) enhance the voltage plateau of the organic materials as cathodes to improve their energy density. (2) use nanotechnology such as method to prepare nanoparticles of these polymer precursors, enlarge their surface area and makes them easier and faster for lithium ion transformation to enhance their performance. (3) Use the special advantage of organic materials of the flexibility to design the next generation of stretchable electrode materials.
(4) Design novel 2D structure conjugated polymers, COFs to increase the activity of carbonyl groups and nitrogen atoms as high-performance electrode materials.

References

[1] L. Yang, Y. Yu, Y. Gong, J. Li, F. Ge, L. Jiang, F. Gao, and Y. Dan. *Polymer Chemistry*. **2015**, 6, 7005-7014.
[2] A. L. Briseno, S. C. Mannsfeld, P. J. Shamberger, F. S. Ohuchi, Z. Bao, S. A. Jenekhe, and Y. Xia. *Chemistry of Materials*. **2008**, 20, 4712-4719.
[3] J. Zhou, X. F. Cheng, B. J. Gao, C. Yu, J. H. He, Q. F. Xu, H. Li, N. J. Li, D. Y. Chen, and J. M. Lu. *Small*. **2019**, 15, 1803896.
[4] J. Zhou, H. Lin, X.-F. Cheng, J. Shu, J.-H. He, H. Li, Q.-F. Xu, N.-J. Li, D.-Y. Chen, and J.-M. Lu. *Materials Horizons*. **2019**, 6, 554-562.
[5] P. Lu, C. Li, E. W. Schneider, and S. J. Harris. *The Journal of Physical Chemistry C*. **2014**, 118, 896-903.
[6] F. A. Soto, Y. Ma, J. M. Martinez de la Hoz, J. M. Seminario, and P. B. Balbuena. *Chemistry of Materials*. **2015**, 27, 7990-8000.
[7] Z. Song, H. Zhan, and Y. Zhou. *Chemical Communications*. **2009**, 448-450.

Chapter 5

A Laddered Structure Polymer as High-performance Electrodes for Lithium-ion Organic Batteries

In this study, a novel strategy for synthesizing organic electrode materials based on dithioether ladder structure has been proposed. By leveraging the interactions of sulfur atoms, the polymer backbone have been successfully reinforced, resulting in improved stability and an ultra-long cycle life over 1000 cycles. Additionally, we carefully investigate the charge-discharge mechanism of this polymer and proposed a bi-functional property in redox reaction and fabricated all-plastic cells based on the property. We then confirm the subsequent charge-discharge mechanism through theoretical calculation and experimental validation in the following characterization and electrochemical experiment. The all-plastic cell shows robust electrochemical performance and provides a feasible strategy to synthesize bi-functional polymers for LIBs.

5.1 Introduction

Rechargeable batteries now play a crucial role in people's daily lives. Since the commercialization of lithium batteries in the 1970s, their production and cost have been constrained by the expensive and scarce lithium resources, as well as the complex and precise manufacturing processes, preventing their widespread application and limiting them to being power sources for high-cost devices. To meet the growing demand for large-scale application of affordable and reliable next-generation energy storage systems, as well as the need for green energy storage, researchers have explored many alternatives to lithium batteries, such as sodium, magnesium, and zinc batteries. Among them, all-plastic batteries have attracted significant attention due to their environmental friendliness and the stable charge-discharge mechanism without lithium metal anodes. Moreover, all-plastic batteries can be used in different electrolyte systems, greatly simplifying the manufacturing process and reducing potential costs. However, current research on all-plastic batteries still faces unresolved challenges, such as the dissolution and degradation of electrode materials, which limit the cycle life of many batteries to fewer than 500 cycles.

In this context, we explored the idea of constructing two-dimensional or even three-dimensional organic polymer frameworks to fabricate large aromatic polymers with strengthened chemical bonds in various dimensions instead of a chain only in one dimension. By leveraging the highly reversible redox reaction from carbonyl groups and aromatic six-membered ring molecular structures of PDB, we created a bi-functional polymers to be applied both as cathode and anode materials in all-plastic cells. This approach successfully led to the development of a novel, stable, and efficient all-plastic electrode material, which demonstrated excellent cycling performance, high energy density, and the ability to charge and discharge at high rates.

5.2 Synthesis and Electrochemical Test

5.2.1 Synthesis of PDB

First, dissolve 0.001 mol (0.2 g) of 2,3,5,6-tetrafluorocyclohexa-2,5-diene-1,4-dione and 10 g of Na2S·9H2O in 50 mL of ethanol while stirring. Then, add 50 mL of deionized water and stir the mixture until uniform. Place the resulting mixture in a water bath at 80°C and heat for 3 hours. During the reaction, add another 50 mL of 2,3,5,6-tetrafluorocyclohexa-2,5-diene-1,4-dione solution and reflux for 10 hours. After the reaction is complete, slowly add dilute hydrochloric acid until a large amount of precipitate forms. Once the precipitation is complete, wash the precipitate sequentially with DMF, ethanol, and deionized water, then dry it in an oven at 60°C for 12 hours to obtain black PDB powder. Fig 5.1 illustrates the synthesis of PDB.

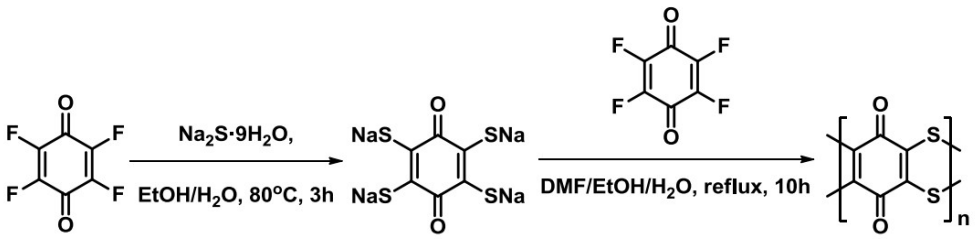

Figure 5.1 Synthesis route of PDB

5.2.2 Electrochemical Measurements of PDB

The assembled coin cells were tested by NEWARE multifunctional battery test systems with galvanostatic charge-discharge in the scope from 1.5 to 3.5V as half-cell and 0-3.0V as all-plastic cell. Charge and discharge curves, cycling stability, rate performances and long-term cycling results can also be obtained. Cyclic voltammetry (CV) parameters are set at a scan rate of 0.1 mV/s via battery CV testing system CV view2 software. For pre-lithiation process, the discharge process was set from 3.5V to 0.005V.

5.3 Results and Discussions

As shown in the SEM images in Fig 5.2, image A depicts the freshly synthesized, untreated PDB particles, which vary in size from 1 to 10μm. After grinding, the PDB particles in the homogeneous slurry are uniformly spherical, with a diameter of around 1μm (image C). The rough protrusions on the surface indicate that the grinding process resulted in a uniform precursor, which plays a crucial role in improving battery performance.

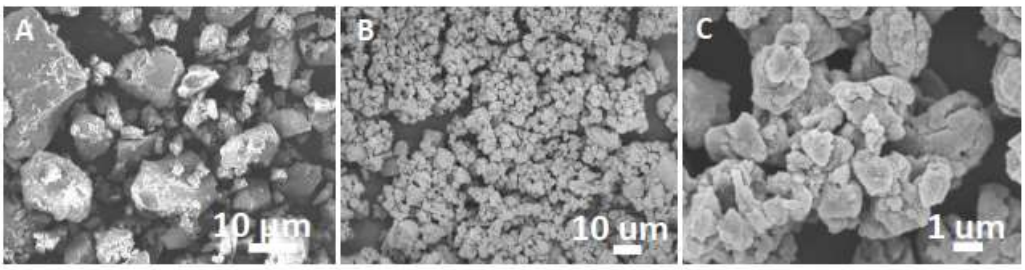

Figure 5.2 SEM images of pristine PDB and as-prepared PDB

FTIR characterization results show a stretching vibration peak for carbonyl functional groups at a wavelength of 1632 cm^{-1}, along with four additional absorption peaks corresponding to the different vibrational modes of the -C-S-C- bond[1-3], as shown in Fig 5.3. This confirms the successful synthesis of the PDB polymer molecules.

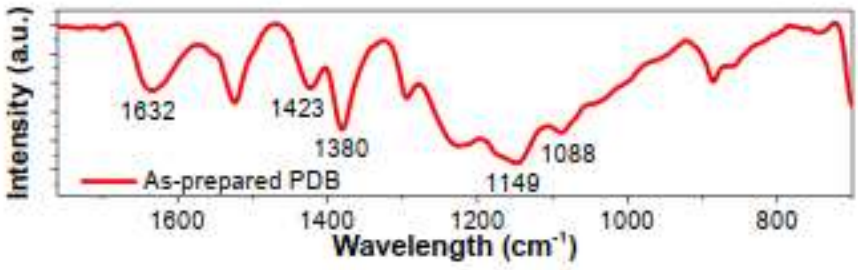

Figure 5.3 FTIR profile of PDB

The TGA analysis results, as shown in Fig 5.4, indicating that PDB molecules exhibit high stability, retaining more than 95% of their weight up to 290°C. Even at 700°C, they still retain 55% of their weight. Considering that the typical operating environment for lithium-

ion batteries ranges from -20°C to 60°C, this demonstrates that PDB is fully suitable as an electrode material for lithium-ion batteries.

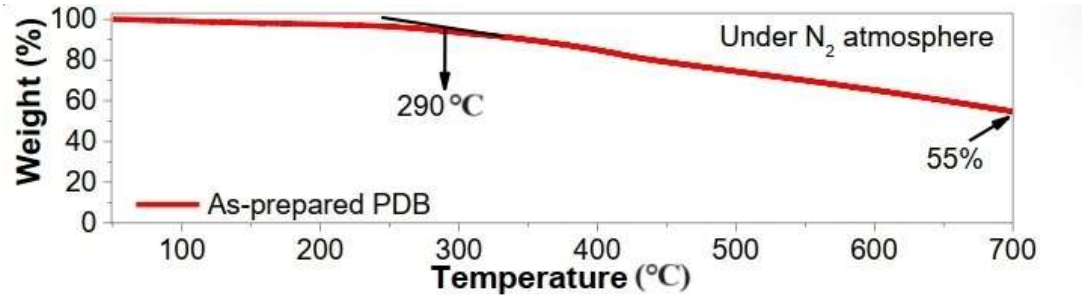

Figure 5.4 PDB weight loss under temperature programming

Elemental analysis experiments determined that the carbon content of PDB is 39.33% and the sulfur content is 37.85%, with a carbon-to-sulfur ratio of 1.04. These results are highly consistent with the theoretical values of 42.85%, 38.13%, and 1.12, respectively, providing preliminary evidence for the successful synthesis of the polymer. The subsequent EDS mapping results (Fig 5.5) show that only trace amounts of sodium and fluorine elements are present in PDB molecules at different locations, while the majority of the polymer chain ends are -SNa, with only a small portion of unreacted -SNa and -F. This further confirms the occurrence of the polymerization reaction, with the resulting average degree of polymerization being 8.

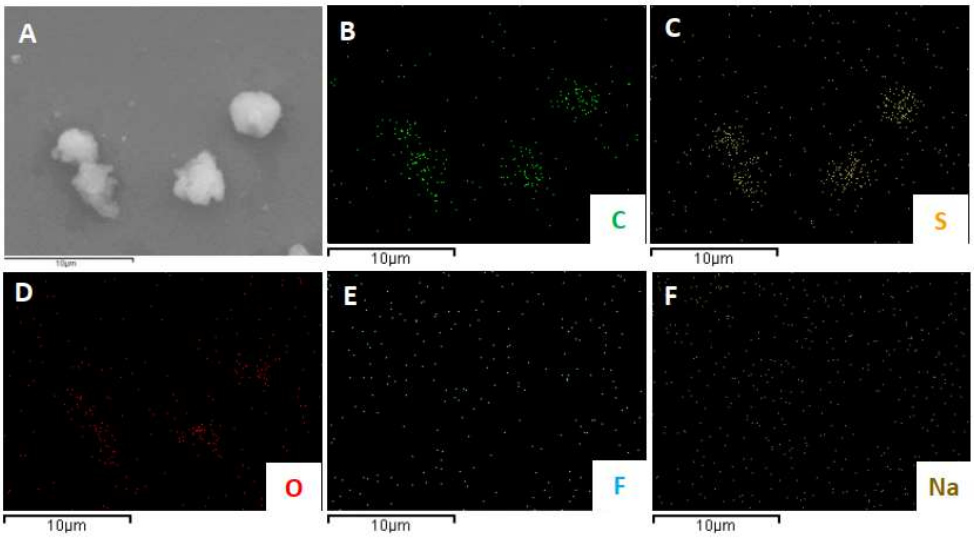

Figure 5.5 EDS mapping of PDB from different areas

To test PDB's performance in different electrolyte systems, it was first applied in a traditional $LiPF_6$ in EC/DEC carbonate electrolyte (Fig 5.6). PDB's capacity quickly declines in carbonate electrolytes, dropping to less than 20% after 20 cycles. This is due to the rapid dissolution of PDB in this electrolyte system, which destabilizes the electrode material. Therefore, a stable LiTFSI in DOL/DME ether-based electrolyte[4-5] was used in subsequent experiments.

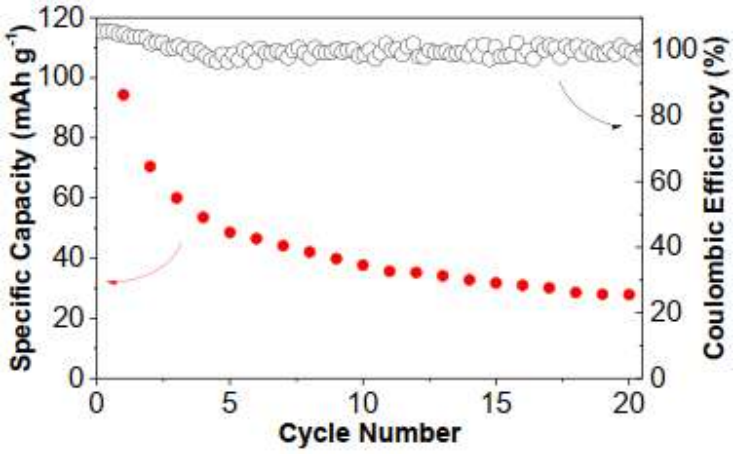

Figure 5.6 Cycle performance of PDB cathodes in $LiPF_6$ in EC/DEC

Electrochemical Impedance Spectroscopy (EIS) characterization was further investigated the compatibility of PDB with ether-based electrolyte. The cell using a carbonate-based electrolyte exhibits a higher internal resistance (149 Ω), significantly exceeding that of the cell with an ether-based electrolyte (28 Ω), with a resistance approximately 5.3 times higher as shown in Fig 5.7. The resistance values were obtained from the semicircles in the high-frequency range. A lower resistance indicates a faster electron transfer rate. This suggests that the ether-based electrolyte demonstrates better compatibility with the PDB electrode compared to the traditional carbonate-based electrolyte.

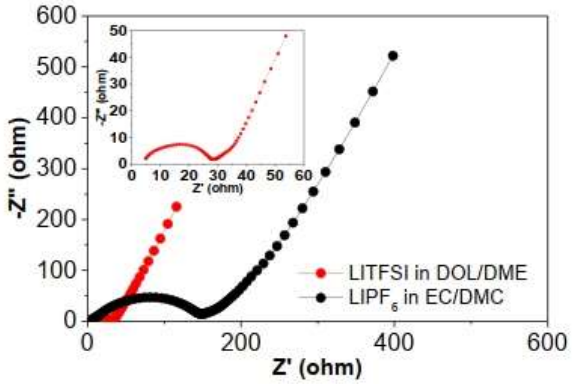

Figure 5.7 Enlarged EIS inset plot of PDB fresh cells with ether-based electrolyte (LiTFSI in DOL/DME) (red) and carbonate-based electrolyte ($LiPF_6$ in EC/DMC) (black)

When used as a cathode material, PDB has a theoretical capacity of 319 mAh/g, with the first-cycle experimental capacity measured at 260 mAh/g. After multiple cycles, it still retains over 200 mAh/g of capacity, indicating that both carbonyl groups on the PDB monomer molecule can serve as active sites for lithium storage. The reaction mechanism of PDB as a cathode material is shown in Fig 5.8a. The charge-discharge curves show that PDB has charge-discharge plateau as a cathode material, with the recharge voltage increasing from 1.5V to 3.5V, and a distinct recharge plateau observed at 2.2V, while the discharge plateau is less pronounced (Fig 5.8b). The cycling performance tests demonstrate that PDB has excellent stability, retaining 95% of its capacity after 100 cycles at a current density of 20 mAh/g, and it can quickly recover to near its initial capacity after charging (Fig 5.8c). Fig 5.8d shows the rate performance of PDB at different current densities, indicating that even at a high current (1500 mAh/g), PDB can still maintain a capacity of

over 150 mAh/g, demonstrating its good electrochemical performance under high-rate charge-discharge conditions.

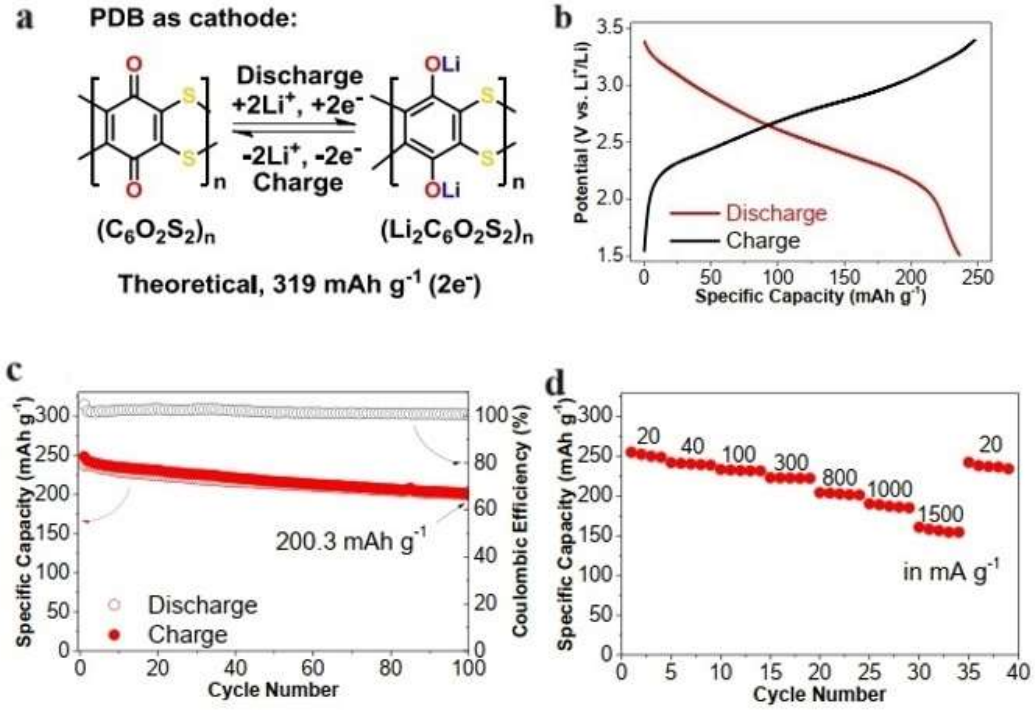

Figure 5.8 a) Mechanism of PDB as cathode b) Charge-discharge profile of PDB c) Cycle performance of PDB in 20 mAh/g d) Rate performance of PDB

The CV test curves (Fig 5.9) show two peaks at 2.43V and 2.92V during charging, and two peaks at 2.30V and 2.90V during discharging, corresponding to the lithium intercalation and de-intercalation of carbonyl groups. The peaks at 3.23V and 3.14V correspond to the oxidation and reduction peaks of sulfur atoms[6]. The high degree of overlap in the curves over three cycles indicates the high reversibility of the redox reactions, confirming that PDB is fully suitable as a cathode material for rechargeable batteries.

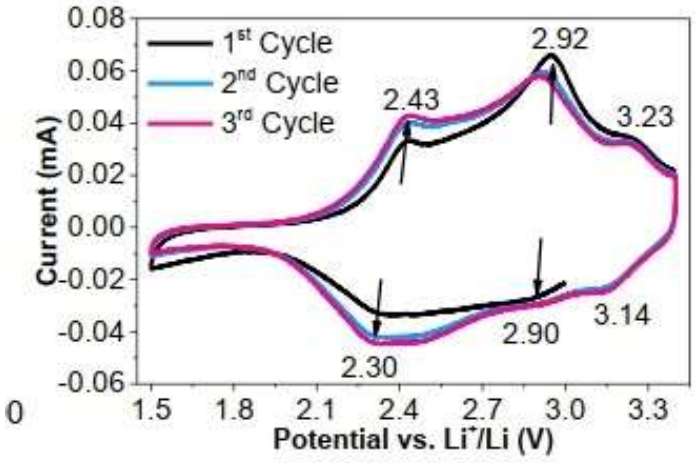

Figure 5.9 CV profile of PDB

The occurrence of the enolization process was further validated through ex-situ FTIR analysis of the PDB electrode at different discharge and charge states (Fig 5.10a). As shown in Fig 5.10b, during the discharge process (3.4V to 1.5V, from point a to point c), the intensity of the absorption peak at approximately 1632 cm^{-1} (highlighted in pink), corresponding to the C=O stretching vibration, gradually decreases. This indicates the reduction or disappearance of C=O groups during lithiation or reduction. Upon charging to 2.5 V (point d), the reappearance of the C=O signal suggests the regeneration of C=O groups during delithiation or oxidation.

Moreover, the absorption peak at approximately 1059 cm^{-1} (highlighted in deep yellow) corresponds to =C-O stretching vibrations (Fig 5.10c). Initially (at point a), the =C-O signal is nearly undetectable. However, during discharge to 1.5 V (from point a to point c), the intensity of the =C-O peak increases, indicating the formation of =C-O groups during lithiation. Conversely, upon charging to 2.5 V (point d), the intensity of the =C-O peak decreases, signifying the reoxidation of =C-O groups back into C=O groups. These results clearly confirm the reversibility and reactivity of the redox-active C=O groups in PDB during lithiation and delithiation processes.

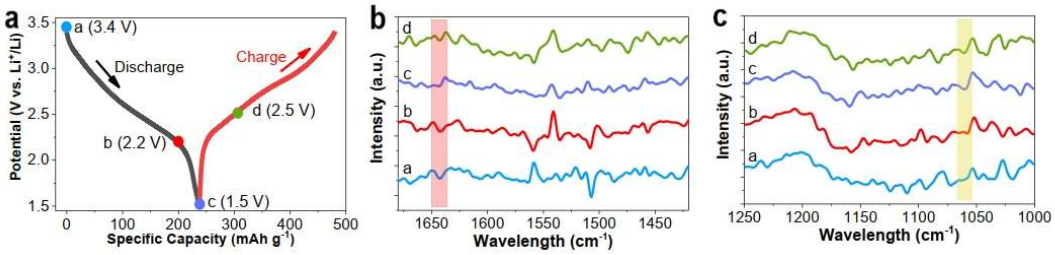

Figure 5.10 Ex-situ FTIR analysis of PDB between 3.4-1.5V. a) Galvanostatic charge and discharge profiles at different discharge and recharge status b) FTIR spectra of C=O groups obtained from disassembled cells c) =C-O groups from disassembled cells

The ultra-long cycle performance test of PDB (Fig 5.11) shows that at a current density of 20 mAh/g, the battery still retains 80.5% of its capacity after 1000 cycles, strongly demonstrating the stability of PDB as a cathode material, with the Coulombic efficiency remaining near 100%, indicating the reversibility of the redox reactions and full utilization of the material.

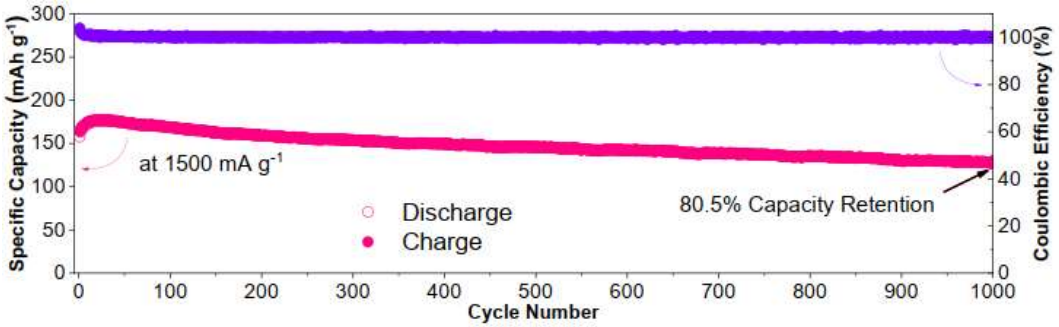

Figure 5.11 Ultra long cycle performance of PDB

Next, PDB was tested as an anode material. Fig 5.12a shows the charge-discharge curves at different cycle numbers, revealing good stability (discharging from 2.8V to 0.005V). The rate performance of PDB at different current densities (Fig 5.12b) shows that it retains good capacity even at 1000 mAh/g, and at an ultra-high current density of 4200 mAh/g, the main lithium-ion intercalation/de-intercalation active sites are on the benzene rings. The cycling performance test (Fig 5.12c) indicates that PDB maintains good stability as an anode material.

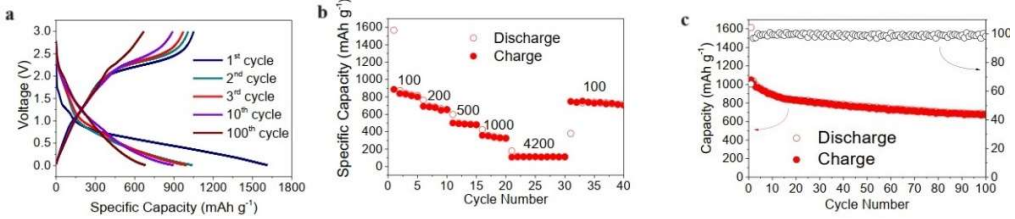

Figure 5.12 a) Specific capacity of PDB under different cycles b) Rate performance of PDB c) Cycle performance of PDB

To further illustrate PDB's performance as an anode material, it was fully discharged to 0.005V and then pre-lithiated[7] (Fig 5.13a), showing a capacity of up to 1600 mAh/g. To eliminate the influence of CNT as a conductive agent, which inherently has some capacity, the capacity of CNT was measured at 48 mAh/g (Fig 5.13b). This shows that the majority of the capacity comes from PDB, confirming its feasibility as an anode material.

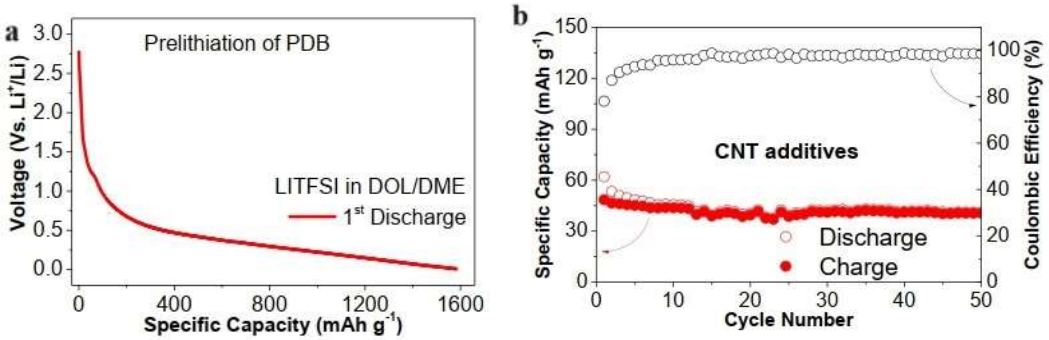

Figure 5.13 a) Prelithiation of PDB discharging from 2.8V to 0.005V b) Capacity of CNT additives

Given that PDB exhibits good electrochemical performance as both cathode and anode material, an all-plastic cell[8] was assembled. The charge-discharge mechanism of PDB as both cathode and anode is illustrated in Fig 5.14a. As a cathode, the carbonyl groups participate in lithium storage; as an anode, both the carbonyl groups and benzene rings are involved in lithium intercalation and deintercalation. The full battery's charge-discharge curve (Fig 5.14b) shows a distinct charging plateau at 1.3V and a discharge plateau above 0.5V when discharging from 3.0V to 0.005V. The rate performance test of the full battery

(Fig 5.14c) indicates that it maintains a high capacity at a current density of 300 mAh/g, but the capacity decreases to 50 mAh/g at a high current density of 1000 mAh/g, indicating that the full battery's tolerance to high-rate charge-discharge is not optimal. The long term cycling performance test (Fig 5.14d) shows that even at a current density of 500 mAh/g, the all-plastic battery retains a capacity of over 100 mAh/g after 250 cycles. Excluding the rapid capacity decline during the initial cycles due to irreversible reactions (such as SEI formation), the subsequent cycles maintain stable capacity, indicating the significant stability of PDB as a full battery electrode material.

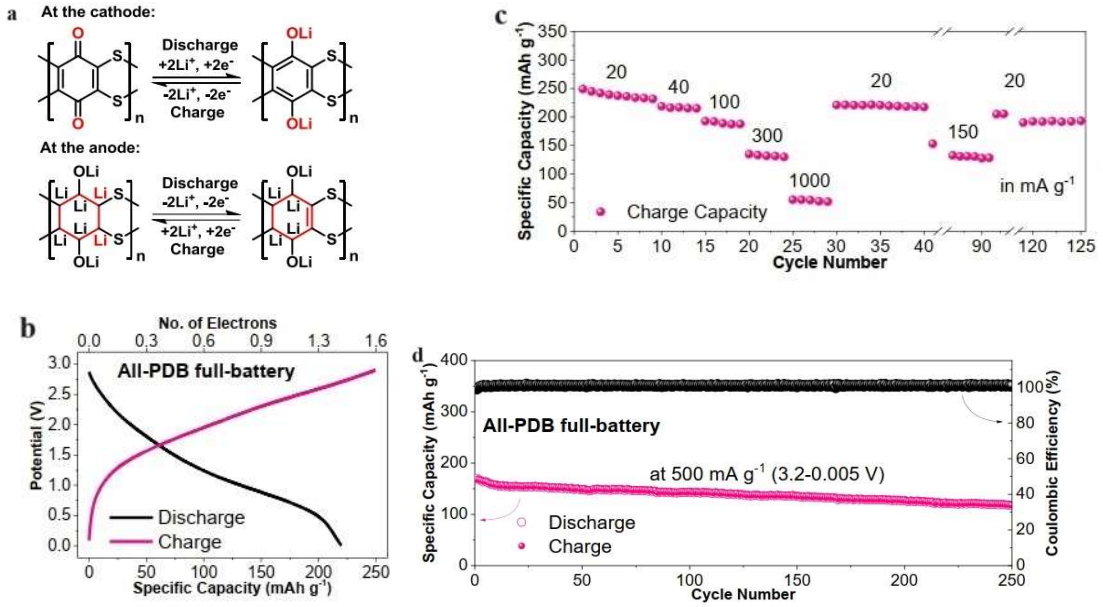

Figure 5.14 a) Mechanisms of PDB as both electrodes b) Charge-discharge profile of full battery c) Rate performance of the full battery d) Long term cycle performance of full battery

In the second part of the experiment, a novel conjugated polymer with a 2D structure was successfully synthesized through a simple condensation reaction. Compared to other organic materials in all-plastic battery systems, this polymer, PDB, stands out as a high-quality organic electrode material due to its exceptionally good cycling performance and stability. Additionally, this part of the experiment delves deeply into the mechanism of the bifunction of the PDB in redox reaction both in cathode and anode during the charge and discharge process to explain their feasibility in both electrodes. Pre-lithiation profiles indicate the successful lithiation of lithium ions in benzene rings and carbonyl groups, thus,

suitable for the application of anode materials to store lithium ions. While on the other hand, the carbonyl groups can also serve as active sites in higher voltage platform in 1.4-3.5V to store and release lithium ions as cathode materials as shown in Fig 5.15.

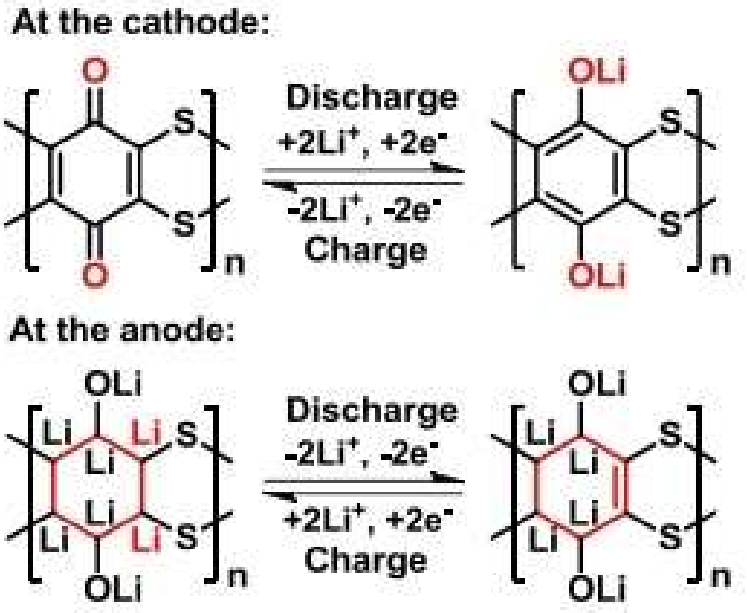

Figure 5.15 PDB during redox reaction in charge/discharge process

Theoretical simulations and FTIR experiments confirmed the mechanism of PDB. Thanks to the unique bi-functional properties of PDB, it can show reversible lithiation/de-lithiation property both on carbonyl groups and benzene rings. This mechanism ensures that during the charging and discharging process, PDB plays an important role of lithium intercalation and de-intercalation in both two electrodes. CV profiles further indicates that carbonyl groups and benzene rings participate in the redox reaction.

The stable chemical structure of PDB enables it to exhibit excellent battery performance when used as a cathode material. It can withstand high-rate currents of 1500 mAh/g and maintain over 80% of its capacity after 1000 cycles of charge and discharge at a current of 20 mAh/g. When used as an anode material, it can still retain a capacity of 180 mAh/g after 1000 cycles at a high current of 2000 mAh/g, which is equivalent to 74% of its initial capacity. The stability of PDB in both the cathode and anode allows the assembled all-

plastic battery to maintain good cycling performance and capacity, holding 176 mAh/g at a current density of 300 mAh/g. Even at a high current of 500 mAh/g, it retains 81% of its initial capacity after 250 cycles, which is among the best performance reported for all-plastic batteries.

However, PDB as both the cathode and anode material in an all-plastic battery still faces some challenges. Firstly, the battery's performance at high voltages is suboptimal, limiting its energy density. Additionally, at ultra-high-rate current densities, the cycling performance deteriorates rapidly, highlighting a significant gap in fast-charging efficiency compared to commercial inorganic batteries. The charge-discharge platform of the all-plastic battery is also not smooth enough, which not only reduces the battery's capacity but also impacts its overall stability. Another issue is the electrolyte, as the battery's capacity quickly declines in commercial carbonate-based electrolytes. These issues require further research to resolve.

As further research progresses, new battery systems with metal-free all-plastic batteries could eventually be suitable candidates to replace lithium-ion batteries, and likely to achieve commercial viability and play unique roles in specific applications.

5.4 Conclusions

We have successfully designed an organic active electrode material based on its bi-function both as anode and cathode material during redox reaction and applied it in all-plastic lithium-ion battery cell, which exhibits exceptionally beneficial cycling performance and energy density with decent rate capacity, with a lifespan of up to 250 cycles still retains 80% of the specific capacity. The battery also withstands high-rate charge and discharge current density at 300 and 1000 mA/g with specific capacity of 135 and 55 mAh/g. Subsequently, theoretical calculations and characterizations further confirmed the stable bifunction and mechanism of this structure during the charge and discharge processes. This work provides a new approach for designing high-performance all-plastic batteries, and it

is believed that with continued research, the performance of all-plastic batteries may eventually rival that of inorganic batteries and ultimately become practical.

References

[1] T. Ma, Q. Zhao, J. Wang, Z. Pan, and J. Chen. *Angewandte Chemie International Edition*. **2016**, 55, 6428-6432

[2] K. Liu, J. Zheng, G. Zhong, and Y. Yang. *Journal of Materials Chemistry*. **2011**, 21, 4125-4131

[3] Z. Song, H. Zhan, and Y. Zhou. *Chemical Communications*. **2009**, 448-450

[4] S. Phadke, M. Cao, and M. Anouti. *ChemSusChem*, **2018**, 11, 965

[5] K. Zhang, C. Guo, Q. Zhao, Z. Niu, and J. Chen. *Advanced Science*. **2015**, 2, 1500018

[6] Z. Song, Y. Qian, T. Zhang, M. Otani, and H. Zhou. *Advanced Science*. **2015**, 2, 1500124

[7] J. Xie, Z. Wang, P. Gu, Y. Zhao, Z. J. Xu, and Q. Zhang. *Science China Materials*. **2016**, 59, 6-11

[8] M.-S. Balogun, W. Qiu, Y. Luo, H. Meng, W. Mai, A. Onasanya, T. K. Olaniyi, and Y. Tong. *Nano Research*. **2016**, 9, 2823-2851

Chapter 6

Conclusions and Recommendations

This chapter provides a comprehensive discussion and summary of the results for the two synthesized classes of conjugated polymers. The following two sections respectively discuss and evaluate the results of the ion-in-conjugation polymer and the laddered structure polymer. Subsequently, the attempt to use PDAS as a binder and to optimize the electrode material is presented, along with the proposal of a new synthesis strategy to further explore potential polymer materials to enhance battery performance. Finally, the chapter discusses the major unresolved issues in organic batteries and proposes related solutions for future research.

6.1 General Discussion

The whole endeavors of this research focus on the synthesis of novel conjugated polymers and the application of different strategies to enhance their potential as electrode materials in rechargeable batteries. Two different classes of conjugated polymer macromolecules are explored in the project, comprehensive characterization and electrochemical testing are conducted to interpret their properties and functions. The charge-discharge mechanisms of the different materials, as well as the methods for improving their performance, are also thoroughly discussed in their respective sections. Finally, this chapter examines the remaining challenges with these two types of materials and recommends the direction for future research.

6.2 Reconnaissance work not included in main chapters

6.2.1 Optimization of PDAS

As the poor intrinsic low potential of both 1,5-PDAS and 2,6-PDAS as cathode materials largely limit their application, PDAS polymers are used as organic novel binder for inorganic system lithium titanate LTO batteries to test their performance. Fig 6.1 shows conventional LTO with super P as conductive agent have a wide and smooth plateau at 1.6V during the recharge process and charge at 1.5 V. LTO as an inorganic anode material is well known for its excellent ultralong stability during cycles and inorganic materials tend to have a smooth plateau during electrochemical performance which indicating they have higher energy density. The pure LTO have the specific capacity at around 120 mAh/g with conventional binder of PVDF. Experiment have investigated PDAS as a good conductive polymer using less conductive agent and even without binder to exhibit their electrochemical performance. Thus, 1,5-PDAS and 2,6-PDAS are applied as active biner for LTO to replace the conventional inactive PVDF.

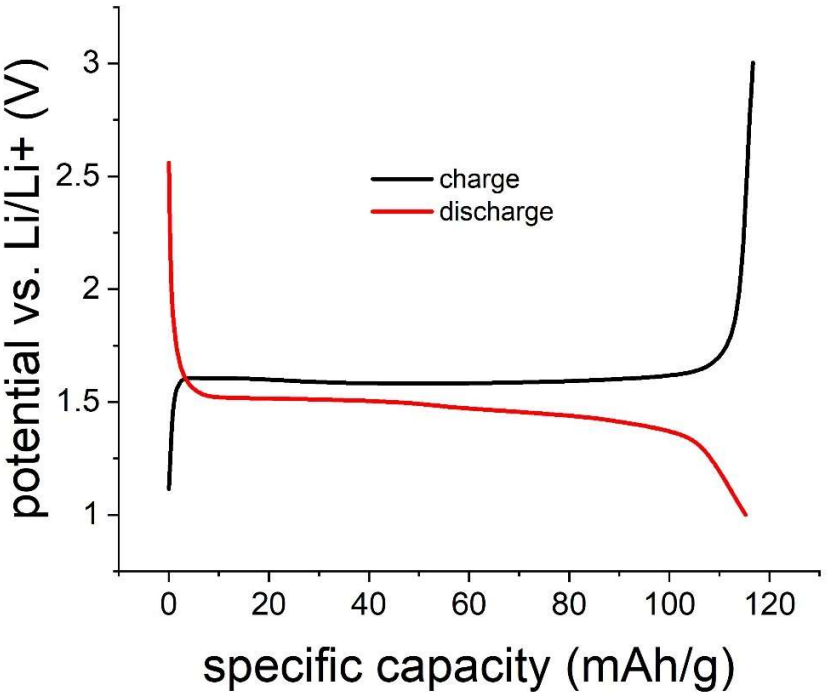

Figure 6.1 The profile diagram of charge and discharge i-V curves of LTO

Fig. 6.2 shows 1,5-PDAS could largely enhance the capacity of LTO, the formula is

LTO: super P : PDAS = 8 : 1 : 1,

although have around 30 mAh/g irreversible capacity coursed by 1,5-PDAS, indicating the low Coulombic efficiency at the initial cycles, the capacity will finally stabilize at 150 mAh/g, which means 1,5-PDAS offer an extra 30 mAh/g of capacity.

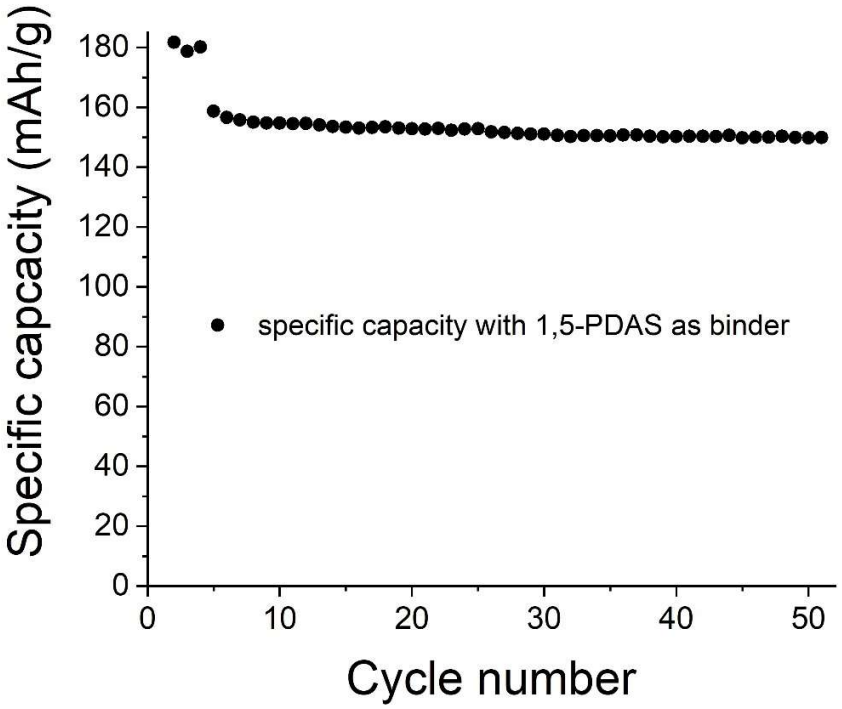

Figure 6.2 The specific capacity of LTO with 1,5-PDAS as binder

Fig 6.3 shows the 2,6- PDAS as an active binder for LTO. 2,6-PDAS have a quite high initial Coulombic efficiency at the initial cycles and thus the specific capacity is stable at around 130mAh/g, the long cyclic performance is not as good as 1,5-PDAS with faster decay of capacity and a lower improvement of capacity at only 10 mAh/g.

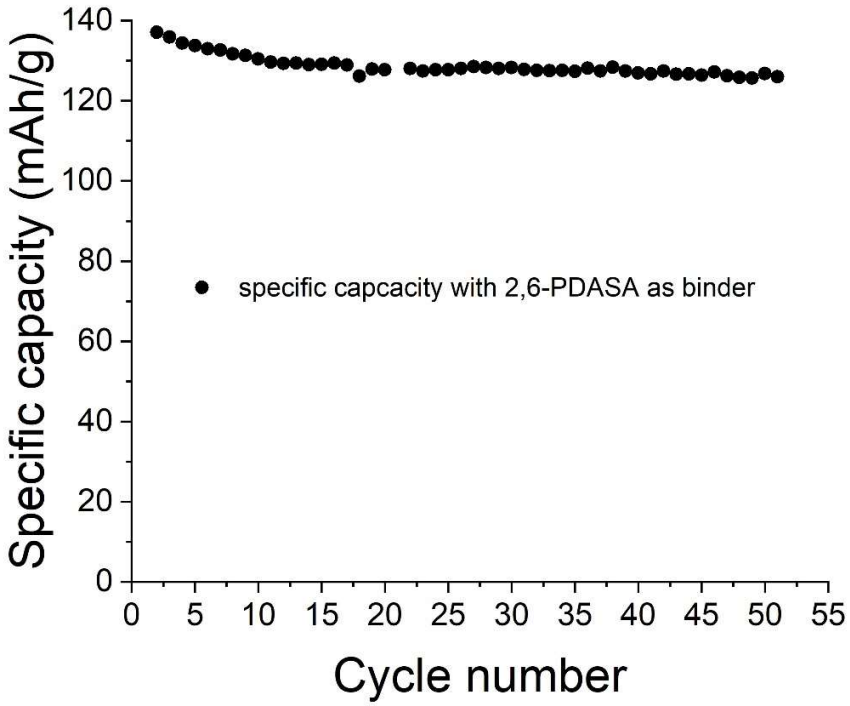

Figure 6.3 The specific capacity of LTO with 2,6-PDAS as binder

There is a synergetic effect of 1,5-PDAS and 2,6-PDAS. The theoretical capacity of the both the polymers indicate they can only enhance the capacity at about 10 mAh/g, however, 1,5-PDAS improve the reversible capacity of LTO at almost 30 mAh/g which is higher than commercial LTO capacity produced in large scale and 2,6-PDAS also improves the performance by 10-15 mAh/g. This demonstrates other parameters have been influenced by the PDAS such as the electrode structure, especially considering the crystalline morphology of 1,5-PDAS, further investigation is needed to figure out the mechanism.

Fig 6.4 shows the SEM image of free-standing LTO with 1,5-PDAS and the electrode exhibit excellent flexibility[3-5], which indicates it can be applied as energy system in flexible device. Further exploration and research project will be followed to fabricate flexible cells and apply them in the flexible device as energy storage system.

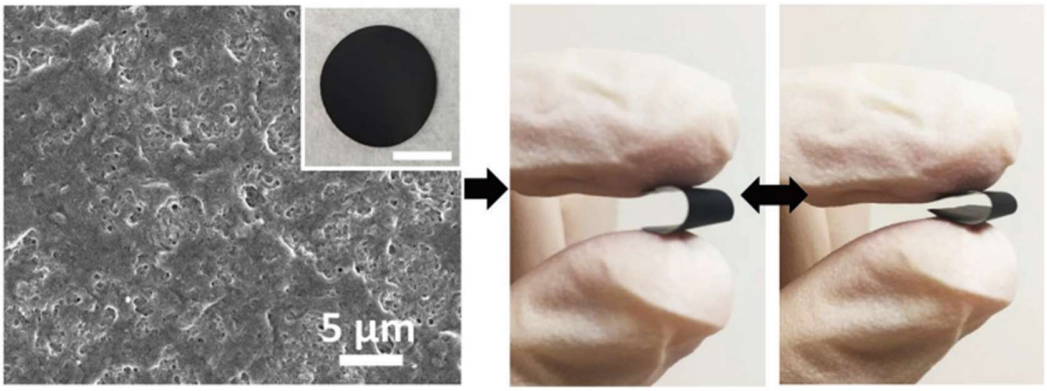

Figure 6.4 SEM image of LTO with 1,5-PDAS and the electrode shows excellent flexibility

6.2.2 Design of Novel 2D Materials as High Performance Electrode

The performance of electrode is largely influenced by the crystallinity and specific surface area of the active material offers an idea to design 2D framework to enhance the capacity of LIBs. 2D structure can improves the stability in electrolyte compared with small molecules and their large surface area provides more active centers for lithium diffusion, which can enhance the rate performance and cyclic stability. N-doped 2D framework is proposed to change the electrochemical properties of the conjugated systems in the center of the nitrogen atoms and adjacent carbon atoms. Research reveals the ability of nitrogen atoms as active centers in electrochemical performance. In addition, nitrogen active centers offer extra static charge impulsion between different layers of 2D materials to avoid stacking and maintain a decent surface area. Fig 6.5 shows inspiration from the excellent electron and ion transformation molecule porphyrin, also friendly for the environment, the "poly-porphyrin" is proposed, and investigations of its electrochemical performance will be studied with further experiment[1-2].

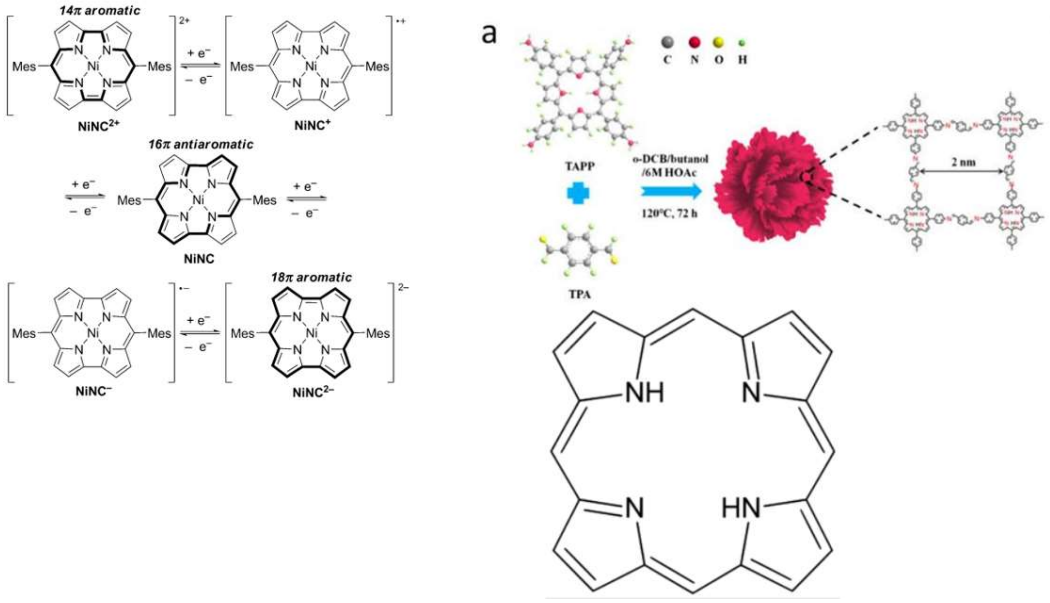

Figure 6.5 Illustration of some porphyrin-like structures and proposed synthesis of 2D frameworks. Reproduced with permission from [2].

6.3 Outstanding Questions

Through decades of research on organic batteries, the performance of organic materials as battery components has gradually reached a level comparable to traditional materials like lithium cobalt oxide, lithium iron phosphate, and lithium nickel cobalt manganese oxide (LiNCM), showcasing unique advantages in many parameters. With continued research, it is believed that organic batteries, and even fully organic batteries, could eventually become widely applicable energy storage devices.

However, there are still significant challenges that need to be addressed before organic batteries, particularly organic electrode materials, can be widely adopted. One major issue is the steep curve observed in the CV profiles of organic batteries during charging and discharging cycles. This indicates that these batteries have a very short, or even nonexistent, charging and discharging voltage plateau. This not only reduces the energy density of the battery but also raises concerns about stability and safety, leading some researchers to classify these systems as pseudo-capacitors rather than true batteries. Therefore, it is crucial to explore methods such as inducing and polarization effects and modifying the electrode

surface to enhance ion transport efficiency and diffusion distance, thereby achieving a more stable charging and discharging plateau.

Another challenge is the generally unsatisfactory conductivity of organic electrode materials, which necessitates the addition of a significant number of conductive agents like CNTs and carbon black. However, these conductive agents have low capacity themselves, reducing the loading of active materials and, consequently, lowering the overall battery capacity. In the first part of the experiment, the use of ion-in-conjugation polymer effectively addressed this issue, but it still required 30% by weight of CNTs for conductivity. In comparison, traditional inorganic batteries typically require less than 10% of conductive agents. Designing high-loading materials, charged electrode materials, and pre-doping ions could help activate the conductivity of organic materials.

Finally, the development of new electrolyte systems should also be pursued in parallel. The two types of polymers synthesized in this experiment exhibited rapid capacity decay in traditional lithium battery electrolytes, such as $LiPF_6$ in carbonate solution, with capacity falling below 80% in less than 20 cycles. Most organic materials do not perform well in traditional electrolytes. Unfortunately, research on electrolytes for organic batteries has lagged significantly behind that for inorganic batteries. Therefore, developing new electrolyte formulations is a crucial direction to explore, as finding the most suitable electrolyte for a given battery system could maximize the performance of organic electrode materials.

References

[1] J. Y. Shin, T. Yamada, H. Yoshikawa, K. Awaga, and H. Shinokubo. *Angewandte Chemie International Edition*. **2014**, 126, 3160-3165

[2] J. Xie, Z. Wang, Z. J. Xu, and Q. Zhang. *Advanced Energy Materials*. **2018**, 8, 1703509

[3] L. Nyholm, G. Nyström, A. Mihranyan, and M. Strømme. *Advanced Materials.* **2011**, *23*, 3751- 3769

[4] J. Wu, X. Rui, G. Long, W. Chen, Q. Yan, and Q. Zhang. *Angewandte Chemie International Edition*. **2015**, 54, 7354-7358

[5] X. Han, G. Qing, J. Sun, and T. Sun. *Angewandte Chemie International Edition*. **2012**, 124, 5237-5241